Chalmers Winter School February 2026

Three lectures

Quantum Geometry in Linear Response

Lecture notes

Raquel Queiroz | Columbia University | Revised November 19, 2026

These lectures derive standard results of linear response, the conductivity and its sum rules, from the point of view of quantum geometry. The final formulas are textbook material, but the language brings a lot of intuition, and it simplifies the mathematics in a way that makes every step transparent. The starting observation is that an electric field can do two things to an electron in a crystal. It can accelerate the electron through its band, which is the process described by the dispersion, or it can change the wave function by mixing it with other bands, and this second process is controlled by the matrix elements of the position operator. Quantum geometry is the way to organize these matrix elements, and it connects them to how much the electrons fluctuate in space.

We follow that connection from the free electron gas to the optical response of a crystal. In the first lecture we construct the quantum geometric tensor by asking how a quantum state changes when we vary a parameter, and we find that when the parameter is the crystal momentum it measures the fluctuations of position. In the second lecture we follow those fluctuations in time, which gives the conductivity and the optical sum rules. In the third lecture we derive the full constraint on the optical weight, and we use bonding, orbital interference and flat bands to understand where the geometry comes from in real materials.

Conventions

The electron charge is $-e$, with $e > 0$, and $\hbar = 1$. Fields vary as $e^{-\mathrm{i}\omega t}$; a retarded response is evaluated at $z = \omega + \mathrm{i}0^+$. The Berry connection is $\mathcal{A}_\mu = \mathrm{i}\langle u|\partial_\mu u\rangle$, so

$$\mathcal{G}_{\mu\nu} = g_{\mu\nu} - \frac{\mathrm{i}}{2}\Omega_{\mu\nu}, \qquad \Omega_{\mu\nu} = \partial_\mu \mathcal{A}_\nu - \partial_\nu \mathcal{A}_\mu.$$

Band-response formulas below describe clean, independent electrons at zero temperature unless stated otherwise. The momentum integral $\int_{\mathrm{BZ}} \frac{\mathrm{d}^d k}{(2\pi)^d}$ gives quantities per physical volume, or per area for a two-dimensional system. Spin and valley multiplicities are included only when their states are explicitly summed. In the cyclotron formulas B is defined by the Lorentz force $-e\,\mathbf{v}\times\mathbf{B}$ (in Gaussian units this B is B_{G}/c). We use Gaussian units for the sheet admittance in the Faraday calculation and for $\epsilon = 1 + 4\pi\chi$.

Contents

1 Lecture 1: From current conservation to position fluctuations 3
1.1 What a free electron can absorb . . . 3
1.2 Following a state through parameter space . . . 4
1.3 Why the projector derivative connects different subspaces . . . 5
1.4 Position in a crystal . . . 6
1.5 Which projector does the experiment select? . . . 7

2 Lecture 2: Geometry, dynamics and optical sum rules 10
2.1 Wannier spread and the trace bound . . . 10
2.2 A Landau level has one dipole frequency . . . 11
2.3 Projected position and anomalous velocity . . . 12
2.4 Velocity differentiates both energies and projectors . . . 13
2.5 Following the dipole fluctuation in time . . . 14
2.6 From fluctuations to the longitudinal response . . . 15
2.7 The transverse response and its sign . . . 17
2.8 The Fermi surface supplies the Drude term . . . 18
2.9 Low and high frequencies probe different moments . . . 19
2.10 One absorption spectrum, several moments . . . 21
2.11 A useful bound and the single-frequency limit . . . 23

3 Lecture 3: Optical weight, bonding and lattice interference 25
3.1 Deriving the f-sum rule . . . 25
3.2 Energy gaps do not determine polarization . . . 27
3.3 From an isolated bond to a chain . . . 28
3.4 Bonding and the location of charge . . . 31
3.5 Orbital interference in a triangular unit . . . 33
3.6 Flat bands from destructive interference . . . 34
3.7 Moiré length scales and what flatness leaves behind . . . 37

A Checks that fix the conventions 38
A.1 One occupied and one empty level . . . 38
A.2 A metal screens with a negative Drude susceptibility . . . 38
A.3 The diamagnetic and paramagnetic terms . . . 38
A.4 A single band and the occupied subspace are different choices . . . 39

B Recordings 39

1 Lecture 1: From current conservation to position fluctuations

1.1 What a free electron can absorb

We start with the simplest possible metal, free electrons with $H = p^2/(2m_e)$, and ask what an electric field does to them. In a spatially uniform field every electron feels the same force,

$$m_e \dot{v}_\mu = -eE_\mu, \qquad j_\mu = -n_e e v_\mu, \tag{1.1}$$

so that the current obeys $\dot{j}_\mu = (n_e e^2/m_e)E_\mu$. A pulse of the field changes the momentum of the electrons, and because nothing in a clean electron gas can take that momentum away, the current it creates stays forever.

∴ **Drude conductivity**

For a harmonic field, $-\mathrm{i}z j_\mu = (n_e e^2/m_e)E_\mu$. Thus

$$\sigma_{\mu\mu}(z) = \frac{\mathrm{i}D}{z}, \qquad D = \frac{n_e e^2}{m_e}. \tag{1.2}$$

The retarded prescription separates dissipation from the reactive response:

$$\frac{\mathrm{i}}{\omega + \mathrm{i}0^+} = \pi\delta(\omega) + \mathrm{i}\,\mathcal{P}\frac{1}{\omega}, \qquad \mathrm{Re}\,\sigma_{\mu\mu}(\omega) = \pi D\delta(\omega). \tag{1.3}$$

All of the optical weight sits at zero frequency, and nothing can be absorbed at any finite frequency. Counting half of the delta function on the positive-frequency axis,

$$\int_0^\infty \mathrm{Re}\,\sigma_{\mu\mu}(\omega)\,\mathrm{d}\omega = \frac{\pi D}{2} = \frac{\pi n_e e^2}{2m_e}. \tag{1.4}$$

The fact that this result survives interactions, for electrons in the continuum with a parabolic kinetic energy, comes from momentum conservation. As long as the interactions depend only on the relative coordinates of the electrons, the total momentum $\mathbf{P}_{\mathrm{tot}} = \sum_i \mathbf{p}_i$ commutes with the Hamiltonian, $[H, \mathbf{P}_{\mathrm{tot}}] = 0$, and because every electron has the same mass the uniform current density is simply proportional to it, $\mathbf{J} = -e\mathbf{P}_{\mathrm{tot}}/(m_e V)$. When two electrons scatter they exchange momentum, but whatever one of them loses the other gains, so the total current cannot relax. In a lattice band this argument no longer holds, because the current carried by an electron is not proportional to its crystal momentum.

The same reasoning applies in a uniform magnetic field. The center of mass still separates from the relative motion of the electrons, so the cyclotron resonance stays at $\omega_c = e|B|/m_e$ however the electrons interact, which is Kohn's theorem Kohn (1961). A magnetic field is therefore a first example of how optical weight can move to a finite frequency without any lattice.

What happens when we add a lattice potential? For electrons in the continuum, with a potential that depends only on position, the integral in Eq. (1.4) does not change. What changes is how this weight is distributed between the peak at zero frequency and the transitions at finite frequency. This is the optical f-sum rule, which we derive in Lecture 3. A good way to think about it is that the integral over all frequencies probes the electrons at very short times, before they have had time to find out about the lattice or about each other, and all that such a measurement can reveal is how many electrons there are and their bare mass. A model that keeps only a few bands sees only part of

this weight, so its restricted optical sum can be smaller than the bare-electron value, which is what an effective mass expresses.

This is the point to keep in mind for the rest of the lectures. Whatever a crystal absorbs at a finite frequency was taken from the peak at zero frequency by the lattice, and it appears at energies set by the crystal potential and by the hopping between orbitals. Impurities also break translation symmetry, but they only broaden the delta function into a peak whose width is the scattering rate, and we do not consider them here. Quantum geometry describes the weight that the lattice moves to finite frequency.

1.2 Following a state through parameter space

Let us leave the electron gas for a moment and ask a general question: what happens to a quantum state when we change a parameter of its Hamiltonian? Let $|\psi(\boldsymbol{\lambda})\rangle$ be a normalized eigenstate that depends smoothly on a set of parameters $\boldsymbol{\lambda}$, which may be a crystal momentum, a twist of the boundary conditions or a slowly varying field. As we move in parameter space we expect the state to rotate, and the natural way to measure by how much is to compare it with its neighbor,

$$|\psi(\boldsymbol{\lambda}+\mathrm{d}\boldsymbol{\lambda})\rangle = |\psi\rangle + |\partial_\mu\psi\rangle \mathrm{d}\lambda_\mu + O(|\mathrm{d}\boldsymbol{\lambda}|^2). \tag{1.5}$$

Because the state stays normalized, $\langle\partial_\mu\psi|\psi\rangle = -\langle\psi|\partial_\mu\psi\rangle$, so this number is purely imaginary, and the overlap between the two states changes at first order only through its phase:

$$\langle\psi(\boldsymbol{\lambda}+\mathrm{d}\boldsymbol{\lambda})|\psi(\boldsymbol{\lambda})\rangle = 1 + \mathrm{i}\mathcal{A}_\mu \mathrm{d}\lambda_\mu + O(|\mathrm{d}\boldsymbol{\lambda}|^2), \qquad \mathcal{A}_\mu = \mathrm{i}\langle\psi|\partial_\mu\psi\rangle. \tag{1.6}$$

The Berry connection $\mathcal{A}_\mu$ is not something we can measure, because we are free to multiply the state by a different phase at every $\boldsymbol{\lambda}$, and under $|\psi\rangle \mapsto e^{\mathrm{i}\alpha}|\psi\rangle$ it changes to $\mathcal{A}_\mu - \partial_\mu\alpha$. What survives is its circulation around a closed loop, where the gauge dependence drops out. This is the Berry phase, defined modulo 2π, and by Stokes' theorem it is the flux through the loop of the Berry curvature Berry (1984), which is gauge invariant at every point of parameter space:

$$\gamma = \oint \mathcal{A}_\mu \mathrm{d}\lambda_\mu, \qquad \Omega_{\mu\nu} = -2\,\mathrm{Im}\langle\partial_\mu\psi|\partial_\nu\psi\rangle. \tag{1.7}$$

This is the usual story, and it concerns the phase that the state accumulates. A second thing happens as we push the state along its path, and it is just as important: part of the state leaks out, in the sense that the new state no longer lies entirely along the old one. A phase cannot reduce the magnitude of the overlap, so the reduction measures the part of $|\partial_\mu\psi\rangle$ that is perpendicular to the original state. To isolate it we introduce the projector onto the state and its complement,

$$P = |\psi\rangle\langle\psi|, \qquad Q = 1 - P, \qquad |D_\mu\psi\rangle = Q|\partial_\mu\psi\rangle. \tag{1.8}$$

Then

$$|\langle\psi(\boldsymbol{\lambda}+\mathrm{d}\boldsymbol{\lambda})|\psi(\boldsymbol{\lambda})\rangle|^2 = 1 - g_{\mu\nu}\mathrm{d}\lambda_\mu\mathrm{d}\lambda_\nu + O(|\mathrm{d}\boldsymbol{\lambda}|^3), \tag{1.9}$$

where $g_{\mu\nu} = \mathrm{Re}\langle D_\mu\psi|D_\nu\psi\rangle$ is the quantum metric Provost and Vallee (1980). In quantum information the same quantity is called the fidelity susceptibility, because it tells us how quickly the state becomes distinguishable from itself as the parameter changes. The remainder is cubic in general because we expanded about one endpoint.

⋆ **The quantum geometric tensor**

The inner products of the perpendicular changes define

$$\mathcal{G}_{\mu\nu} = \langle \partial_\mu \psi | Q | \partial_\nu \psi \rangle = g_{\mu\nu} - \frac{\mathrm{i}}{2}\Omega_{\mu\nu}. \tag{1.10}$$

Its real, symmetric part is the metric, which measures how much the state itself changes, and its imaginary, antisymmetric part is the curvature, which measures the phase accumulated when changes in two directions are combined. Under a gauge change the vector $Q|\partial_\mu\psi\rangle$ only acquires the phase $e^{\mathrm{i}\alpha}$, so its inner products are gauge invariant. The metric and the curvature are two parts of the same object.

A large metric means that nearby values of the parameter correspond to states that are easy to tell apart. Whether a drive in time actually causes transitions depends, in addition, on how fast the parameter changes compared with the excitation gaps.

1.3 Why the projector derivative connects different subspaces

Working with a state forces us to carry its arbitrary phase around. There is a better way, which uses only gauge-independent objects from the start, and that is to ask how the projector changes. The projector does not have the phase problem, because the phase of the ket cancels against that of the bra. It also makes precise what we mean when we say that the state leaks out: it leaks into the complement Q, which contains every state outside P. To see this, differentiate $P^2 = P$:

$$(\partial_\mu P)P + P(\partial_\mu P) = \partial_\mu P. \tag{1.11}$$

Multiplying by P on both sides gives $P(\partial_\mu P)P = 0$, and multiplying by Q gives $Q(\partial_\mu P)Q = 0$. The derivative of the projector therefore has no part inside the subspace and no part inside its complement, and all that is left are the two blocks that connect them:

$$\partial_\mu P = P(\partial_\mu P)Q + Q(\partial_\mu P)P. \tag{1.12}$$

This is the statement to remember: the change of a projector points entirely out of the subspace. The derivative of a particular state can still have a component along the state, which is its change of phase, and the projector does not see it.

∴ **The QGT in projector form**

For a single state,

$$(\partial_\mu P)|\psi\rangle = |\partial_\mu\psi\rangle + |\psi\rangle\langle\partial_\mu\psi|\psi\rangle \tag{1.13}$$
$$= |\partial_\mu\psi\rangle - |\psi\rangle\langle\psi|\partial_\mu\psi\rangle = Q|\partial_\mu\psi\rangle. \tag{1.14}$$

Therefore

$$\mathcal{G}_{\mu\nu} = \mathrm{Tr}[P(\partial_\mu P)(\partial_\nu P)]. \tag{1.15}$$

Using Eq. (1.12) and cyclicity of the trace,

$$g_{\mu\nu} = \frac{1}{2}\,\mathrm{Tr}[(\partial_\mu P)(\partial_\nu P)], \tag{1.16}$$
$$\Omega_{\mu\nu} = \mathrm{i}\,\mathrm{Tr}\{P[\partial_\mu P, \partial_\nu P]\}. \tag{1.17}$$

> Nothing in these formulas requires P to project onto a single state. They define the metric and curvature, traced over the group, for any set of bands that varies smoothly, and the bands inside the group may cross each other as long as the whole group stays separated from the states we excluded. To define a quantum geometric tensor we therefore need only two things: the set of states we care about and the parameter we change.

1.4 Position in a crystal

Let us go back to materials, where the natural parameter is the crystal momentum. A Bloch eigenstate $|\psi_{n\mathbf{k}}\rangle = e^{i\mathbf{k}\cdot\mathbf{r}}|u_{n\mathbf{k}}\rangle$ extends through the whole sample, so position is a delicate operator in a periodic system, and we have to be careful about how it acts.

Differentiating the Bloch factor with respect to $\mathbf{k}$ brings down a factor of $\mathbf{r}$, which gives

$$r_\mu|\psi_{n\mathbf{k}}\rangle = -i\partial_{k_\mu}|\psi_{n\mathbf{k}}\rangle + ie^{i\mathbf{k}\cdot\mathbf{r}}|\partial_{k_\mu}u_{n\mathbf{k}}\rangle. \tag{1.18}$$

Position acting on a Bloch state is therefore a derivative with respect to crystal momentum, plus a second term that we must keep, in which the derivative acts on the cell-periodic part. If we insert this in a wave packet, integrate the first term by parts in $\mathbf{k}$ and project onto the Bloch basis, we find that position acts on the band amplitudes as Blount (1962)

$$[r_\mu]_{nm} = i\delta_{nm}\partial_{k_\mu} + \mathcal{A}_\mu^{nm}(\mathbf{k}), \qquad \mathcal{A}_\mu^{nm} = i\langle u_n|\partial_{k_\mu}u_m\rangle. \tag{1.19}$$

The first term moves the wave packet within its band. In the second, the diagonal elements are the Berry connection of each band, which is gauge dependent, and the off-diagonal elements $r_\mu^{nm} = \mathcal{A}_\mu^{nm}$, $n \neq m$, are the dipole matrix elements between bands, the amplitudes for a dipole transition.

The quantum geometric tensor keeps only the off-diagonal part, so the gauge-dependent piece never enters. For one isolated band, inserting a complete set of states gives

$$\begin{aligned}\mathcal{G}_{\mu\nu}^n &= \sum_{m\neq n} r_\mu^{nm} r_\nu^{mn} \\ &= \langle\partial_\mu u_n|(1 - |u_n\rangle\langle u_n|)|\partial_\nu u_n\rangle.\end{aligned} \tag{1.20}$$

The derivative of the wave function in momentum space and the dipole matrix elements in real space therefore describe the same quantity. If there were only one band there would be no complement to leak into, position would cause no transitions, and we would be back to the electron gas of the first section.

Figure 1 shows the two views of the same change of wave function. Moving to a neighboring momentum changes the occupied state, and the component of that change in the other band is the dipole amplitude that an electric field couples to.

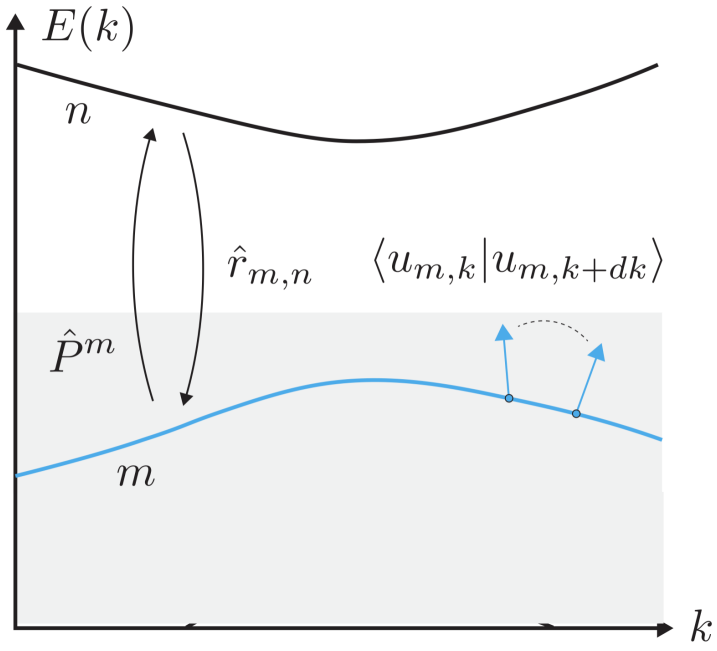


Figure 1: The change of a Bloch state and its interband dipole. The blue arrows are cell-periodic states at nearby momenta. Their overlap measures how much the state changes. The black arrows indicate the complementary-band matrix element r^{mn}; in a two-band problem its squared magnitude gives the metric of the selected band. Here the selected band is labeled m (shaded) and its complement is labeled n.

1.5 Which projector does the experiment select?

We said that the tensor can be defined for any set of states, so which projector should we use? The experiment decides. In a band insulator, optical absorption takes an electron from an occupied state to an empty one, and a transition into a state that is occupied is blocked by the Pauli principle. The projector that matters is therefore the one onto all the occupied bands, $P(\mathbf{k}) = \sum_{n\in\text{occ}} |u_n\rangle\langle u_n|$, and its quantum geometric tensor contains only the dipole matrix elements between occupied and empty states:

$$\mathcal{G}^{\text{occ}}_{\mu\nu}(\mathbf{k}) = \sum_{\substack{n\in\text{occ}\\ m\in\text{emp}}} r^{nm}_{\mu} r^{mn}_{\nu}. \tag{1.21}$$

Figure 2 illustrates what happens when we fill one more level at fixed $\mathbf{k}$. The middle level changes roles: it can now supply an electron to the upper level, and an electron from below can no longer enter it.

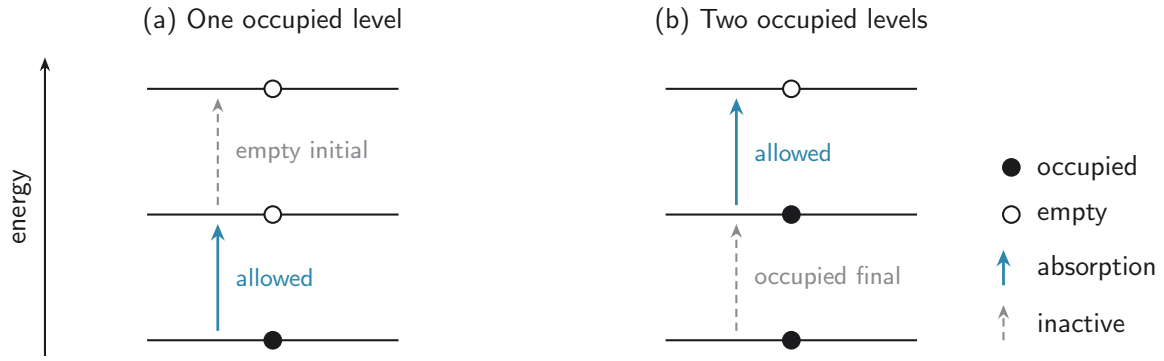


Figure 2: The levels and their dipole matrix elements are the same in both panels. Only neighboring levels are dipole coupled in this example. At zero temperature an upward transition from n to m carries the occupation factor $f_n(1-f_m)$. Only the solid arrow has weight in each panel.

The picture of fluctuations is exact for a finite Slater determinant, where Wick's theorem gives the covariance of the many-electron position $X_\mu = \sum_i r_{i\mu}$ as

$$\langle \delta X_\mu \delta X_\nu \rangle = \mathrm{Tr}[P r_\mu Q r_\nu]. \tag{1.22}$$

For a finite sample with open boundaries, X_μ and X_ν commute, so this covariance is real and symmetric. Multiplying by e^2 gives the covariance of the electric dipole. In a periodic crystal we instead twist the boundary conditions, shifting every crystal momentum by the same amount. The real part of the resulting bulk tensor measures the spread of position; its imaginary part gives the integrated Berry curvature and can be nonzero even though the finite-sample covariance is real. Per electron it has units of length squared, so it defines a length, the geometric length ℓ_g of Fig. 3, which is a scale hidden in the wave functions and absent from the band energies.

∴ Why the many-electron fluctuation contains an empty-state projector

Take a finite Slater determinant and any one-particle operators A, B. Their many-particle lifts are $\widehat{A} = \sum_{ij} A_{ij} c_i^\dagger c_j$ and $\widehat{B} = \sum_{kl} B_{kl} c_k^\dagger c_l$. Choose an occupied/empty basis, with $\langle c_i^\dagger c_j \rangle = f_i \delta_{ij}$ and $f_i \in \{0, 1\}$. Wick contraction gives

$$\langle c_i^\dagger c_j c_k^\dagger c_l \rangle - \langle c_i^\dagger c_j \rangle \langle c_k^\dagger c_l \rangle = f_i(1-f_j)\delta_{il}\delta_{jk}. \tag{1.23}$$

Multiplying by the matrix elements and summing,

$$\langle \delta\widehat{A}\, \delta\widehat{B} \rangle = \sum_{ij} f_i(1-f_j) A_{ij} B_{ji} = \mathrm{Tr}(PAQB), \qquad Q = 1 - P. \tag{1.24}$$

For $A = B = x$, this is $\sum_{i\in\mathrm{occ}, j\in\mathrm{emp}} |x_{ij}|^2$. Transitions between two occupied orbitals drop out because the final orbital is blocked, so the variance of the many-electron position is smaller than the sum of the variances of the individual orbitals, which would include those transitions. The contraction is exact for a finite system. For a periodic bulk system the position operator has to be replaced by the twist of the boundary conditions described in the text.

In a metal the story changes, because the occupation jumps at the Fermi surface. The projector onto the occupied states is then discontinuous as a function of momentum, the correlations in real

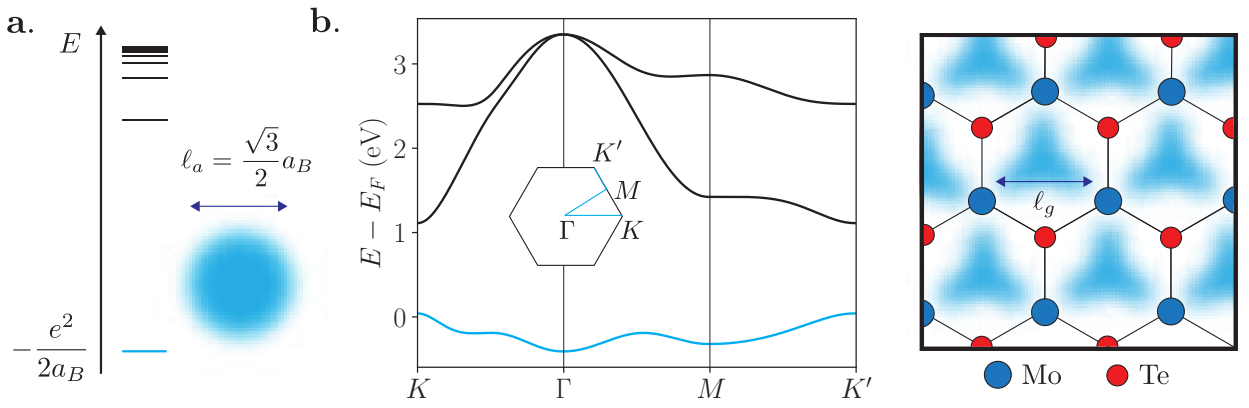


Figure 3: Atomic and crystalline length scales ℓ_a and ℓ_g: an atomic level diagram beside a model band structure and its charge distribution in real space. The interband matrix elements set the spread of the occupied subspace.

space decay as a power law instead of exponentially, and the position fluctuation of the ground state diverges in the thermodynamic limit. This divergence is how Kohn distinguished a metal from an insulator: a state that is infinitely sensitive to a twist of the boundary conditions is truly delocalized Kohn (1964). The interband matrix elements are still there and remain useful, and the part of the response that comes from the Fermi surface is the Drude term of Lecture 2.

2 Lecture 2: Geometry, dynamics and optical sum rules

2.1 Wannier spread and the trace bound

We ended the first lecture with two ways of looking at the same quantity. We can ask how fast the Bloch state of a band changes with momentum, or we can add up the dipole transitions from that band to all the others, and the answer is the same: the larger the dipole fluctuations are in real space, the faster the state changes in momentum space. A first consequence is that the metric sets a minimum size for anything we build out of the band. If we construct Wannier functions for an isolated group of bands, their total quadratic spread separates into a gauge-invariant part and a nonnegative part that depends on the choice of gauge Marzari and Vanderbilt (1997). In d dimensions,

$$\Omega_I = V_{\text{cell}} \int_{\text{BZ}} \frac{\mathrm{d}^d k}{(2\pi)^d} \operatorname{tr} g^{\text{occ}}(\mathbf{k}), \qquad \Omega_{\text{Wannier}} \geq \Omega_I. \tag{2.1}$$

Here the trace is over the spatial directions and the spread is summed over the Wannier functions of the group in one cell, so dividing by their number gives a spread per orbital. Whatever gauge we choose, the Wannier functions cannot be made smaller than the integrated metric allows, and the localization sum rule connects this minimum size to optical absorption Souza et al. (2000). In more than one dimension the minimum total spread can still contain a gauge-dependent contribution on top of Ω_I.

The metric and the curvature are also not independent of each other. The quantum geometric tensor is a matrix of inner products, a Gram matrix, so it is positive semidefinite, and for two parameter directions this means

$$\det \begin{pmatrix} g_{xx} & g_{xy} - \mathrm{i}\Omega_{xy}/2 \\ g_{xy} + \mathrm{i}\Omega_{xy}/2 & g_{yy} \end{pmatrix} \geq 0. \tag{2.2}$$

Writing out the determinant, and using the inequality between the arithmetic and the geometric mean for the trace, we find Roy (2014)

$$g_{xx} g_{yy} - g_{xy}^2 \geq \frac{\Omega_{xy}^2}{4}, \qquad g_{xx} + g_{yy} \geq |\Omega_{xy}|. \tag{2.3}$$

A band with Berry curvature therefore cannot have an arbitrarily small metric. A good way to think about it is that the curvature is a kind of vorticity of the wave function, and to accommodate a vorticity the state needs some room: there is no such thing as vorticity in a delta function.

Integrating over the Brillouin zone turns this into a statement about topology. For an isolated band in two dimensions with Chern number $C = (2\pi)^{-1} \int_{\text{BZ}} \Omega_{xy} \mathrm{d}^2 k$,

$$\frac{A_{\text{cell}}}{(2\pi)^2} \int_{\text{BZ}} \operatorname{tr} g \, \mathrm{d}^2 k \geq \frac{A_{\text{cell}} |C|}{2\pi}. \tag{2.4}$$

A Chern band therefore has a minimum size, set by its Chern number, and the same topology forbids a smooth periodic gauge for its Bloch states and with it an exponentially localized orthonormal Wannier basis. The integrated metric itself stays finite. When the trace inequality in Eq. (2.3) holds as an equality at every momentum the band is called ideal, and the next section shows the simplest example.

∴ **The entire two-band QGT from one Pauli trace**

Let $H = \mathbf{d}\cdot\boldsymbol{\sigma}$ with $|\mathbf{d}| > 0$, and occupy the lower band. Set $\mathbf{n} = \mathbf{d}/|\mathbf{d}|$, so $P_- = (1 - \mathbf{n}\cdot\boldsymbol{\sigma})/2$ and $\partial_\mu P_- = -(\partial_\mu \mathbf{n})\cdot\boldsymbol{\sigma}/2$. The identity

$$(\mathbf{a}\cdot\boldsymbol{\sigma})(\mathbf{b}\cdot\boldsymbol{\sigma}) = (\mathbf{a}\cdot\mathbf{b})1 + \mathrm{i}(\mathbf{a}\times\mathbf{b})\cdot\boldsymbol{\sigma} \tag{2.5}$$

reduces the projector formula to

$$\mathcal{G}_{\mu\nu} = \mathrm{Tr}(P_-\partial_\mu P_-\partial_\nu P_-) \tag{2.6}$$

$$= \frac{1}{4}\left[\partial_\mu\mathbf{n}\cdot\partial_\nu\mathbf{n} - \mathrm{i}\mathbf{n}\cdot(\partial_\mu\mathbf{n}\times\partial_\nu\mathbf{n})\right]. \tag{2.7}$$

Thus $g_{\mu\nu} = \partial_\mu\mathbf{n}\cdot\partial_\nu\mathbf{n}/4$ and $\Omega_{\mu\nu} = \mathbf{n}\cdot(\partial_\mu\mathbf{n}\times\partial_\nu\mathbf{n})/2$ for the lower band, and we never had to choose a gauge for the eigenvector.
In two dimensions there is a stronger statement. Both derivatives of $\mathbf{n}$ are tangent to the unit sphere, so their cross product is parallel to $\mathbf{n}$, and the Gram determinant is

$$\det g = \frac{|\partial_x\mathbf{n}\times\partial_y\mathbf{n}|^2}{16} = \frac{\Omega_{xy}^2}{4}. \tag{2.8}$$

The determinant bound is therefore saturated for every smooth two-band map. The trace bound need not be:

$$(\mathrm{tr}\, g)^2 - \Omega_{xy}^2 = (g_{xx} - g_{yy})^2 + 4g_{xy}^2. \tag{2.9}$$

It is saturated only when $g_{xx} = g_{yy}$ and $g_{xy} = 0$, that is, when the two tangent vectors have equal length and are orthogonal in these momentum coordinates. Every two-band model saturates the determinant bound automatically, and an ideal band needs this additional condition.

2.2 A Landau level has one dipole frequency

The simplest problem we have at hand, the hydrogen atom of quantum geometry, is a Landau level. The band is completely flat, there is no Fermi velocity, and the only length in the problem is the magnetic length ℓ_B, which therefore determines the metric, the Berry curvature and everything else. To see how, we decompose the position of the electron into a guiding-center coordinate and a cyclotron coordinate. For a completely filled lowest level the guiding-center part only moves electrons among occupied states, while the cyclotron part connects the level $n = 0$ to $n = 1$, and this is the part that Q selects.

Position connects only adjacent Landau levels, with the matrix elements of a harmonic oscillator,

$$|\langle 1|x|0\rangle| = |\langle 1|y|0\rangle| = \frac{\ell_B}{\sqrt{2}}, \qquad \ell_B^2 = \frac{1}{e|B|}. \tag{2.10}$$

The amplitudes for x and y differ by a phase of $\pm\pi/2$, whose sign is set by the orientation of the field, so that per occupied orbital

$$g_{xx} = g_{yy} = \frac{\ell_B^2}{2}, \qquad g_{xy} = 0, \qquad |\Omega_{xy}| = \ell_B^2. \tag{2.11}$$

The symmetric and the antisymmetric parts have the same magnitude, so the trace bound is saturated and the Landau level is ideal. Physically, only one circular polarization can raise the cyclotron oscillator, so the optical selection rule and the equality in Eq. (2.3) express the same chirality. There

is also a single transition, at the single energy ω_c, and this will make the Landau level the reference case for everything that follows.

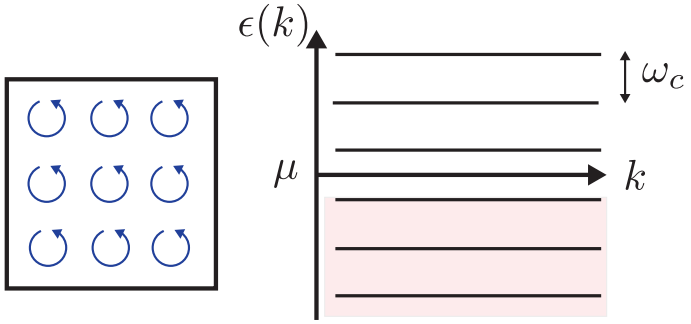


Figure 4: Cyclotron orbits and Landau levels. The pink region marks occupied levels below μ; the horizontal levels indicate the guiding-center degeneracy. Their separation is $\omega_c = e|B|/m_e$ in the $\hbar = 1$ convention. For the filled lowest level discussed here, guiding-center motion remains in the occupied subspace, and the empty-state projector selects the cyclotron transition to the next level.

2.3 Projected position and anomalous velocity

What are the consequences of the geometry if we restrict ourselves to a single band? Projected onto one band, position is the covariant derivative $R_\mu = \mathrm{i}\partial_{k_\mu} + \mathcal{A}_\mu$ of Eq. (1.19). The derivatives commute with each other and so do the connections, but the cross terms do not, and the two components of the projected position fail to commute by the Berry curvature:

$$[R_\mu, R_\nu] = \mathrm{i}\Omega_{\mu\nu}. \tag{2.12}$$

This is the exact analog of the guiding centers of a Landau level, which fail to commute by ℓ_B^2. To see what it does, apply a uniform electric field, which adds a potential linear in position, so that the projected Hamiltonian is $H_{\mathrm{proj}} = \varepsilon_n(\mathbf{k}) + eE_\nu R_\nu$. The Heisenberg equation of motion then gives the velocity Karplus and Luttinger (1954); Xiao et al. (2010)

$$\dot{R}_\mu = \mathrm{i}[H_{\mathrm{proj}}, R_\mu] = \partial_{k_\mu}\varepsilon_n + eE_\nu\Omega_{\mu\nu}. \tag{2.13}$$

The first term is the usual band velocity. The second is the anomalous velocity, perpendicular to the field, which exists only because the projected position operators do not commute. Multiplying by the charge and summing over the occupied states gives the intrinsic Hall response

$$\sigma_{xy}(0) = -e^2 \int_{\mathrm{BZ}} \frac{\mathrm{d}^d k}{(2\pi)^d} \sum_{n\in\mathrm{occ}} \Omega^n_{xy}. \tag{2.14}$$

For a two-dimensional insulator this is $-e^2C/(2\pi)$ in the stated curvature convention Thouless et al. (1982). Even an insulator can therefore carry a current, perpendicular to the field, and its conductivity does not depend on the gap at all: it is fixed by a topological invariant. Notice that the metric played no role in this argument, which is the reason it received so little attention for a long time. As long as we stay within one band, only the curvature enters the semiclassical motion. The metric appears when we allow the field to mix the band with the others, in the polarization and in the absorption at finite frequency.

From geometry to response. Up to here the geometry was static: a spread, a bound, a commutator. In the rest of this lecture we follow the same matrix elements in time, and to do so we take a route

that is different from the standard one. The usual derivation of the conductivity couples the vector potential to the Hamiltonian and expands to second order, which produces a paramagnetic term, a correlation function of currents, and a diamagnetic term (Appendix A.3). It is an algorithm that gives the correct result, but it gives little intuition about where the response comes from. Here we do linear response in real space instead, with correlation functions of position. The reason this is rarely done is the gauge dependence of the position operator, but Lecture 1 showed which of its matrix elements are well defined in a periodic system: the off-diagonal ones.

2.4 Velocity differentiates both energies and projectors

We first need the relation between velocity and position. Let us write the Bloch Hamiltonian in terms of its energies and projectors,

$$H(\mathbf{k}) = \sum_n \varepsilon_n(\mathbf{k}) P_n(\mathbf{k}). \tag{2.15}$$

The velocity is the derivative of the Hamiltonian with respect to momentum, $v_\mu = \partial_{k_\mu} H$. This holds in a complete continuum Bloch representation and in a tight-binding representation that includes the physical positions of the orbitals; in a general momentum-dependent basis the derivative must be read as a covariant one. Differentiating the spectral decomposition gives two terms,

$$v_\mu = \sum_n (\partial_\mu \varepsilon_n) P_n + \sum_n \varepsilon_n \partial_\mu P_n. \tag{2.16}$$

The first is the velocity of each band, from the slope of its dispersion. The second comes from the change of the projectors, which is the leakage out of each band that we met in Lecture 1, and it contains all the matrix elements of the velocity between different bands.

> ∴ **Interband velocity and dipole matrix elements**
>
> Differentiate $H|u_m\rangle = \varepsilon_m |u_m\rangle$ and multiply by $\langle u_n|$, with $n \neq m$:
>
> $$\langle u_n | \partial_\mu H | u_m \rangle = (\varepsilon_m - \varepsilon_n) \langle u_n | \partial_\mu u_m \rangle. \tag{2.17}$$
>
> Defining $\Delta_{mn} = \varepsilon_m - \varepsilon_n$ gives
>
> $$v_\mu^{nm} = -\mathrm{i}\Delta_{mn} r_\mu^{nm}, \qquad v_\mu^{nm} v_\nu^{mn} = \Delta_{mn}^2 \mathcal{G}_{\mu\nu}^{nm}, \quad \mathcal{G}_{\mu\nu}^{nm} = r_\mu^{nm} r_\nu^{mn}. \tag{2.18}$$
>
> Its real and imaginary parts are the metric and curvature of one pair of bands, $\mathcal{G}_{\mu\nu}^{nm} = g_{\mu\nu}^{nm} - \frac{\mathrm{i}}{2}\Omega_{\mu\nu}^{nm}$. An interband current matrix element contains both the transition energy and the dipole fluctuation. Knowing the dispersion alone does not determine it.

As long as we look at matrix elements between different bands, we can therefore think of velocity and position interchangeably: they differ only by the transition energy. The two terms of the velocity are also the two ways in which an electric field acts on a crystal. It can change the occupations within a partially filled band, or it can mix different bands. Figure 5 shows where each process appears in an absorption spectrum, and it is useful to read the spectrum as a sequence of snapshots of the electron at different time scales. At the highest energies the transitions are those of the atom itself, the same dipole transitions that give an atomic orbital its size. At energies of the order of the hopping the electron has had time to spread over neighboring sites, and transitions appear between bands made of the same orbitals, which have no counterpart in a single atom. At the lowest frequencies, in a metal, the electron moves through the whole crystal and we see the Drude peak. A model that keeps only the low-energy bands keeps only the corresponding part of the spectrum.

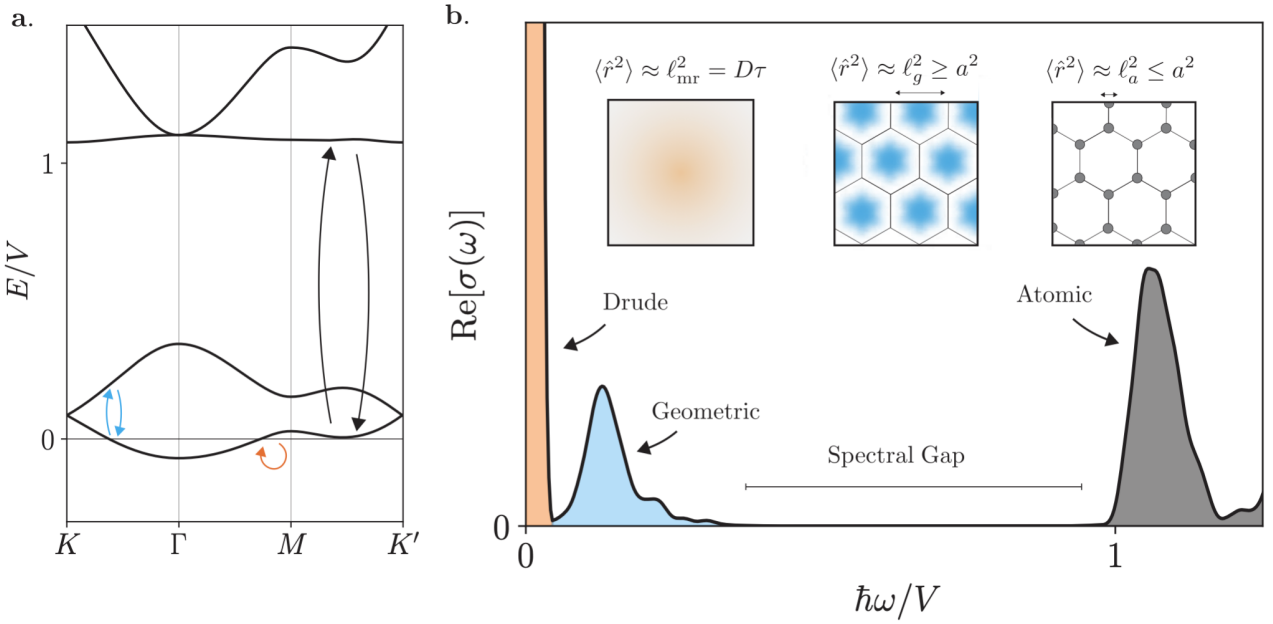


Figure 5: Where optical weight comes from. The orange zero-frequency contribution is intraband motion; the blue finite-frequency part comes from transitions within the low-energy band manifold; the gray peak represents higher-energy atomic transitions. The upper sketches connect these energy scales to spatial structure. "Geometric" labels the low-energy interband sector; higher-energy dipole transitions also contribute to the full position fluctuation. In the sketch, $D\tau$ is a squared diffusion length. Here D denotes the diffusivity.

2.5 Following the dipole fluctuation in time

The quantum geometric tensor is a fluctuation of position, and whenever an operator fluctuates there is a response associated with it; this is the content of the fluctuation–dissipation theorem. To obtain the response we need to know how the fluctuation propagates in time, so instead of the correlation of position with itself at equal times we take it at two different times. Evolving one of the position operators with the Hamiltonian multiplies each matrix element by the phase $e^{-\mathrm{i}\Delta_{mn}t}$, where $\Delta_{mn} > 0$ for occupied n and empty m, and we define the time-dependent quantum geometric tensor per volume as

$$\mathcal{Q}_{\mu\nu}(t) = \int_{\mathrm{BZ}} \frac{\mathrm{d}^d k}{(2\pi)^d} \sum_{\substack{n\in\mathrm{occ} \\ m\in\mathrm{emp}}} e^{-\mathrm{i}\Delta_{mn}t} \mathcal{G}^{nm}_{\mu\nu}. \tag{2.19}$$

At $t = 0$, $\mathcal{Q}_{ij}(0)$ is the localization tensor in the volume normalization used here. Its real part is the integrated occupied-state metric. Its imaginary part is $-\frac{1}{2}\int_{\mathrm{BZ}} \frac{\mathrm{d}^d k}{(2\pi)^d} \sum_{\substack{n\in\mathrm{occ} \\ m\in\mathrm{emp}}} \Omega^{nm}_{ij}$ and retains the bulk curvature. Dividing its diagonal component by the electron density gives the directional mean-square localization length, $\ell_x^2 = \mathcal{Q}_{xx}(0)/n_e$. At later times it is a correlation function of position that is gauge invariant, in which every allowed dipole transition oscillates at its own energy Verma and Queiroz (2025a). Its symmetric part, made of the metric, will give the longitudinal response, and its antisymmetric part, made of the curvature, will give the Hall response.

The simplest insulator is again the filled lowest Landau level, where every allowed transition has the energy ω_c. If the density of the level is n_{LL},

$$\mathcal{Q}_{xx}(t) = n_{\mathrm{LL}} \frac{\ell_B^2}{2} e^{-\mathrm{i}\omega_c t}. \tag{2.20}$$

All the electrons oscillate at one frequency: the size of the fluctuation sets the amplitude and the cyclotron gap sets the frequency. In a crystal the bands disperse, the amplitude and the frequency vary with momentum and with the pair of bands, and $\mathcal{Q}(t)$ is a superposition of many frequencies. A gap sets the lowest of them, and their spread makes the oscillations dephase.

2.6 From fluctuations to the longitudinal response

Now the response. An electric field couples to the electrons through $H' = eE_x(t)X_x$, where $-eX_x$ is the total electric dipole, and what it creates is a polarization $P_x = -e\langle X_x\rangle/V$. Linear response gives the change of the polarization as the retarded commutator of position with itself Kubo (1957), with a step function for causality:

$$\chi_{xx}(t) = \frac{\mathrm{i}e^2}{V}\Theta(t)\langle[X_x(t), X_x(0)]\rangle = \mathrm{i}e^2\Theta(t)[\mathcal{Q}_{xx}(t) - \mathcal{Q}_{xx}(-t)]. \tag{2.21}$$

The last equality holds for an insulator, with the volume normalization absorbed in $\mathcal{Q}$. At equal times $\mathcal{Q}_{xx}(0)$ measures the dipole fluctuation per volume in units of e^2. To get the response to a field applied at time zero, we take the difference between the two time orderings shown above. For $t > 0$ this selects $-2e^2 \operatorname{Im}\mathcal{Q}_{xx}(t)$. Since $\mathcal{G}^{nm}_{xx} = g^{nm}_{xx}$ is real, only the metric enters the longitudinal response:

$$\chi_{xx}(t) = 2e^2\Theta(t)\int_{\mathrm{BZ}}\frac{\mathrm{d}^d k}{(2\pi)^d}\sum_{\substack{n\in\mathrm{occ}\\ m\in\mathrm{emp}}} g^{nm}_{xx}\sin(\Delta_{mn}t). \tag{2.22}$$

∴ Polarizability, conductivity and absorption

The retarded Fourier transform uses

$$\int_0^\infty e^{\mathrm{i}zt}\sin(\Delta t)\,\mathrm{d}t = \frac{\Delta}{\Delta^2 - z^2}, \qquad \operatorname{Im} z > 0. \tag{2.23}$$

Therefore

$$\chi_{xx}(z) = 2e^2\int_{\mathrm{BZ}}\frac{\mathrm{d}^d k}{(2\pi)^d}\sum_{\substack{n\in\mathrm{occ}\\ m\in\mathrm{emp}}}\frac{\Delta_{mn}g^{nm}_{xx}}{\Delta^2_{mn} - z^2}, \tag{2.24}$$

$$\sigma^{\mathrm{inter}}_{xx}(z) = -\mathrm{i}z\chi_{xx}(z) = \mathrm{i}e^2\int_{\mathrm{BZ}}\frac{\mathrm{d}^d k}{(2\pi)^d}\sum_{\substack{n\in\mathrm{occ}\\ m\in\mathrm{emp}}}\Delta_{mn}g^{nm}_{xx}\left(\frac{1}{z-\Delta_{mn}} + \frac{1}{z+\Delta_{mn}}\right). \tag{2.25}$$

The current is the time derivative of the polarization, so the conductivity is the time derivative of the polarizability, which in frequency is the factor $-\mathrm{i}z$. For positive frequency the absorptive part is

$$\boxed{\operatorname{Re}\sigma^{\mathrm{inter}}_{xx}(\omega) = \pi e^2\int_{\mathrm{BZ}}\frac{\mathrm{d}^d k}{(2\pi)^d}\sum_{\substack{n\in\mathrm{occ}\\ m\in\mathrm{emp}}}\Delta_{mn}g^{nm}_{xx}\delta(\omega - \Delta_{mn}).} \tag{2.26}$$

Each transition contributes its energy times the square of its dipole matrix element, and every term is nonnegative, as absorption must be.

Think of two transitions with the same dipole matrix element but different excitation energies. They contribute equally to the position fluctuation. A slowly varying field admixes the lower of the

two excited states into the ground state more easily, so that transition carries more of the static polarizability. When the induced dipole changes in time, we measure a current. At frequencies below the optical gap there is no absorption and the response is purely reactive,

$$\chi_{xx}(0) = 2e^2 \int_{\mathrm{BZ}} \frac{\mathrm{d}^d k}{(2\pi)^d} \sum_{\substack{n\in\mathrm{occ} \\ m\in\mathrm{emp}}} \frac{g_{xx}^{nm}}{\Delta_{mn}}, \qquad \sigma_{xx}^{\mathrm{inter}}(\omega) = -\mathrm{i}\omega\chi_{xx}(0) + O(\omega^3). \tag{2.27}$$

An insulator polarizes without carrying a longitudinal dc current. The static susceptibility has two ingredients: a state that is extended in space has large dipole matrix elements, and a small gap makes the same fluctuation easier to induce. Both enter the intrinsic capacitance of an insulator Komissarov et al. (2024), and in Lecture 3 we will see that the first is the one that distinguishes materials with the same gap.

∴ Switch on a constant field: the metric sets the transient motion

Take a gapped insulator of independent electrons and switch on a constant field, $E_x(t) = E_0\Theta(t)$. Convolving the retarded dipole kernel with the field gives, for $t > 0$,

$$P_x(t) - P_x(0) = E_0 \int_0^t \chi_{xx}(s)\,\mathrm{d}s \tag{2.28}$$

$$= 2e^2 E_0 \int_{\mathrm{BZ}} \frac{\mathrm{d}^d k}{(2\pi)^d} \sum_{\substack{n\in\mathrm{occ} \\ m\in\mathrm{emp}}} \frac{g_{xx}^{nm}}{\Delta_{mn}}[1 - \cos(\Delta_{mn}t)], \tag{2.29}$$

$$j_x(t) = 2e^2 E_0 \int_{\mathrm{BZ}} \frac{\mathrm{d}^d k}{(2\pi)^d} \sum_{\substack{n\in\mathrm{occ} \\ m\in\mathrm{emp}}} g_{xx}^{nm} \sin(\Delta_{mn}t) = -2e^2 E_0\,\mathrm{Im}\,\mathcal{Q}_{xx}(t). \tag{2.30}$$

The current after the step follows the dipole fluctuation directly Verma and Queiroz (2025b). With a single transition the current oscillates forever in this clean model. For a smooth continuum of transition frequencies, each transition still oscillates, but as their phases spread out, their currents cancel. Since current is the rate of change of polarization, the induced polarization then settles to the constant $\chi_{xx}(0)E_0$. A finite discrete spectrum can retain oscillations and recurrences.

Expanding at short times gives

$$j_x(t) = 2e^2 E_0 t \int_{\mathrm{BZ}} \frac{\mathrm{d}^d k}{(2\pi)^d} \sum_{\substack{n\in\mathrm{occ} \\ m\in\mathrm{emp}}} \Delta_{mn} g_{xx}^{nm} + O(t^3). \tag{2.31}$$

For the complete continuum spectrum of an insulator, the f-sum rule identifies the coefficient as $n_e e^2 E_0/m_e$. This is the short-time statement of Lecture 1 seen in real time: at the very beginning the electrons accelerate with their bare mass, as if they were free, and only later do they find out that they are bound and that their motion is limited to a polarization. The expansion requires the corresponding spectral moments to exist, and a model truncated to a few bands has its own optical-weight coefficient.

2.7 The transverse response and its sign

So far we kept only the metric. Weighting the two poles of each transition by the full complex tensor gives the bulk interband transport conductivity,

$$\sigma^{\text{inter}}_{\mu\nu}(z) = \mathrm{i}e^2 \int_{\text{BZ}} \frac{\mathrm{d}^d k}{(2\pi)^d} \sum_{\substack{n\in\text{occ}\\ m\in\text{emp}}} \Delta_{mn} \left[\frac{\mathcal{G}^{nm}_{\mu\nu}}{z-\Delta_{mn}} + \frac{\mathcal{G}^{nm}_{\nu\mu}}{z+\Delta_{mn}} \right]. \tag{2.32}$$

This is what the standard current-response formula gives after using Eq. (2.18), so nothing has been lost by working with position, and for $\mu = \nu$ it reduces to the longitudinal result. Everything that the lattice does to the response is in this expression. Its symmetric part is governed by the metric and its antisymmetric part by the curvature:

$$\sigma^{S}_{\mu\nu}(z) = -2\mathrm{i}e^2 z \int_{\text{BZ}} \frac{\mathrm{d}^d k}{(2\pi)^d} \sum_{\substack{n\in\text{occ}\\ m\in\text{emp}}} \frac{\Delta_{mn} g^{nm}_{\mu\nu}}{\Delta^2_{mn} - z^2}, \tag{2.33}$$

$$\sigma^{A}_{\mu\nu}(z) = -e^2 \int_{\text{BZ}} \frac{\mathrm{d}^d k}{(2\pi)^d} \sum_{\substack{n\in\text{occ}\\ m\in\text{emp}}} \frac{\Delta^2_{mn} \Omega^{nm}_{\mu\nu}}{\Delta^2_{mn} - z^2}. \tag{2.34}$$

The dc limit of the second line reproduces the Hall conductivity of Eq. (2.14), which we obtained from the anomalous velocity of a single band. In the time domain the two pieces combine into a single expression,

$$\sigma^{\text{inter}}_{\mu\nu}(t) = \mathrm{i}e^2 \Theta(t) \partial_t [\mathcal{Q}_{\mu\nu}(t) - \mathcal{Q}_{\nu\mu}(-t)]. \tag{2.35}$$

The bracket exchanges the spatial indices and reverses time together. The conductivity is the rate of change of the position correlation function, and this one line contains the whole interband Kubo formula.

In Eq. (2.35) the time derivative acts only on the correlator. Differentiating the step function as well would add a contact term with Fourier transform $e^2 \int_{\text{BZ}} \frac{\mathrm{d}^d k}{(2\pi)^d} \sum_{\substack{n\in\text{occ}\\ m\in\text{emp}}} \Omega^{nm}_{\mu\nu}$. In the transverse channel this would cancel the dc Hall conductivity: the static dipole of a finite sample cannot carry a steady transport current. In the longitudinal channel the equal-time commutator vanishes, so the two derivatives agree.

∴ Circular absorption measures the trace and the curvature

How would we measure the two parts separately? With circularly polarized light. Choose the complex field amplitudes $\mathbf{e}_\pm = (\hat{\mathbf{x}} \pm \mathrm{i}\hat{\mathbf{y}})/\sqrt{2}$, which fix our convention for the labels + and −. For an occupied state n and an empty state m, write $a = r^{mn}_x$ and $b = r^{mn}_y$. The matrix element for absorption is

$$d^{mn}_\pm = \frac{a \pm \mathrm{i}b}{\sqrt{2}}, \qquad a^* b = \mathcal{G}^{nm}_{xy} = g^{nm}_{xy} - \frac{\mathrm{i}}{2}\Omega^{nm}_{xy}. \tag{2.36}$$

The squared modulus includes the interference between the two dipole amplitudes:

$$|d^{mn}_\pm|^2 = \frac{1}{2}\left(|a|^2 + |b|^2 \mp 2\,\mathrm{Im}[a^* b]\right) \tag{2.37}$$

$$= \frac{1}{2}\left(g^{nm}_{xx} + g^{nm}_{yy} \pm \Omega^{nm}_{xy}\right). \tag{2.38}$$

Let $A_\pm(\omega)$ denote the absorptive conductivity for these unit polarization vectors. For $\omega > 0$,

$$A_\pm(\omega) = \frac{\pi e^2}{2} \int_{\mathrm{BZ}} \frac{\mathrm{d}^d k}{(2\pi)^d} \sum_{\substack{n\in\mathrm{occ} \\ m\in\mathrm{emp}}} \Delta_{mn} \left(g_{xx}^{nm} + g_{yy}^{nm} \pm \Omega_{xy}^{nm} \right) \delta(\omega - \Delta_{mn}). \tag{2.39}$$

The sum removes the handedness; the difference removes the metric:

$$\int_0^\infty \frac{A_+ + A_-}{\omega} \,\mathrm{d}\omega = \pi e^2 \int_{\mathrm{BZ}} \frac{\mathrm{d}^d k}{(2\pi)^d} \sum_{\substack{n\in\mathrm{occ} \\ m\in\mathrm{emp}}} (g_{xx}^{nm} + g_{yy}^{nm}), \tag{2.40}$$

$$\int_0^\infty \frac{A_+ - A_-}{\omega} \,\mathrm{d}\omega = \pi e^2 \int_{\mathrm{BZ}} \frac{\mathrm{d}^d k}{(2\pi)^d} \sum_{\substack{n\in\mathrm{occ} \\ m\in\mathrm{emp}}} \Omega_{xy}^{nm}. \tag{2.41}$$

For a filled group of bands in two dimensions the last momentum integral is $C/(2\pi)$, so the difference equals $e^2 C/2$ in our units. This is the quantized circular-dichroism sum rule (Tran et al., 2017). Since both $|d_\pm|^2$ are positive, we also recover $\operatorname{tr} g^{nm} \geq |\Omega_{xy}^{nm}|$ directly, and we see what saturation means: one of the two circular dipole amplitudes vanishes. The trace condition is an optical selection rule.

2.8 The Fermi surface supplies the Drude term

Everything so far was for an insulator. If a band is partially filled there is an additional contribution, because the field can also change which states of the band are occupied. In a clean metal the distribution function obeys the collisionless equation

$$\partial_t \delta f_{n\mathbf{k}} - eE_\nu \partial_{k_\nu} f_{n\mathbf{k}} = 0. \tag{2.42}$$

At frequency z this gives $\delta f = \mathrm{i} eE_\nu \partial_{k_\nu} f / z$. Multiplying by the current $-ev_\mu^n$ of each state and integrating over momentum, we find

$$\sigma_{\mu\nu}^{\mathrm{intra}}(z) = \frac{\mathrm{i} D_{\mu\nu}}{z}, \qquad D_{\mu\nu} = e^2 \int_{\mathrm{BZ}} \frac{\mathrm{d}^d k}{(2\pi)^d} \sum_n \left(-\frac{\partial f}{\partial \varepsilon_n} \right) v_\mu^n v_\nu^n. \tag{2.43}$$

At zero temperature $-\partial f/\partial\varepsilon = \delta(\varepsilon - \mu)$, so the Drude weight is a property of the Fermi surface, and it vanishes in an insulator. Integrating by parts over the Brillouin zone writes the same quantity as the band curvature of all the occupied states,

$$D_{\mu\nu} = e^2 \int_{\mathrm{BZ}} \frac{\mathrm{d}^d k}{(2\pi)^d} \sum_n f_n \partial_\mu \partial_\nu \varepsilon_n. \tag{2.44}$$

In time, the Drude response is a step, $D_{\mu\nu}\Theta(t)$: the current created by a pulse never decays. In the language of the position correlator it corresponds to adding a term linear in time, $-\mathrm{i} D_{\mu\nu} t/(2e^2)$, to $\mathcal{Q}_{\mu\nu}(t)$ in Eq. (2.35). This gives a simple picture of the three cases. In an insulator the charge only oscillates around its position, at the frequencies of the interband transitions. In a metal with a single band and no interband transitions it only drifts, at a rate set by the Drude weight. In a real metal it does both: it bounces around and drifts at the same time. The linear term is a convenient way to represent the part that grows, and it should not be read as a finite position variance of the metal at equal times, which diverges as we saw in Lecture 1. The full conductivity is the sum of Eq. (2.43) and the interband response.

The Fermi surface fixes the Drude term, but it does not fix how much of the optical weight is left for the interband transitions. A good example is the kagome lattice with nearest-neighbor hopping Verma and Queiroz (2026). Its bands have two van Hove fillings, at $\mu = -2t$ and $\mu = 0$ (hopping amplitude $-t$, $t > 0$), with identical Fermi surfaces (Fig. 6), and looking at the dispersion alone one would treat the two in the same way. The two dispersive bands are mirror images about $-t$, so their velocities reverse on the common Fermi surface and their clean Drude weights coincide. Yet the interband absorption is stronger at the filling next to the flat band: there the Drude weight is 0.46 of the total optical weight, against 0.57 at its partner. The reason is that the Bloch states at the two saddle points are different, and so are the dipole transitions that the Pauli principle leaves open, so the polarization fluctuations differ, and next to the flat band more of the charge stays bound.

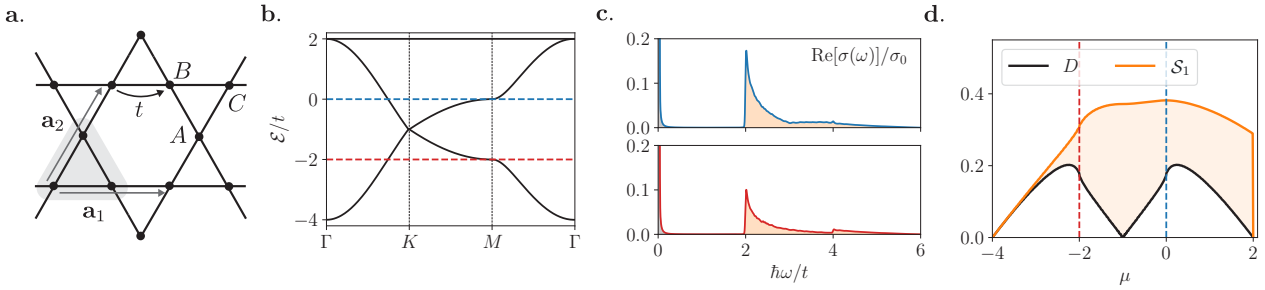


Figure 6: Two van Hove fillings of the kagome metal, from Verma and Queiroz (2026). (a) Lattice with sublattices A, B, C and hopping t. (b) Bands, with the flat band at $2t$ and the van Hove fillings at $\mu = -2t$ (red) and $\mu = 0$ (blue). (c) Optical conductivity at the two fillings: the Drude peaks nearly coincide and the interband absorption (shaded) is stronger at $\mu = 0$. (d) Drude weight D and total weight $\mathcal{S}_1$ against μ. The shaded difference is the weight of the bound charge.

2.9 Low and high frequencies probe different moments

Suppose we drive an insulator below its optical gap and measure the current in direction i from a field in direction j. No real interband transition is available, but the field still polarizes the electrons and can drive a transverse current. To see the two effects in the same measurement, expand the full tensor $\sigma_{ij} = \sigma^S_{ij} + \sigma^A_{ij}$ from Eq. (2.32). Write $\int_{\mathbf{k}} = \int_{\mathrm{BZ}} \frac{\mathrm{d}^d k}{(2\pi)^d}$ and let $\sum'_{nm}$ run over occupied n and empty m. With $z = \omega + \mathrm{i}0^+$ and $|z| \ll \Delta_{\min}$, the expansion is

$$\sigma_{ij}(z) = \underbrace{-e^2 \int_{\mathbf{k}} \sum'_{nm} \Omega^{nm}_{ij}}_{\sigma^A_{ij}(0)} - \mathrm{i}z \underbrace{2e^2 \int_{\mathbf{k}} \sum'_{nm} \frac{g^{nm}_{ij}}{\Delta_{mn}}}_{\chi_{ij}(0)} + z^2 \underbrace{\left(-e^2 \int_{\mathbf{k}} \sum'_{nm} \frac{\Omega^{nm}_{ij}}{\Delta^2_{mn}}\right)}_{h^{(2)}_{ij}} + O(z^3). \tag{2.45}$$

dc Hall conductivity — static polarizability — quadratic Hall dispersion

Equivalently, in terms of the measured coefficients,

$$\sigma_{ij}(z) = \sigma^A_{ij}(0) - \mathrm{i}z\chi_{ij}(0) + z^2 h^{(2)}_{ij} + O(z^3). \tag{2.46}$$

A constant field drives the dc Hall current, with $\sigma^A_{xy}(0) = -e^2 C/(2\pi)$ in two dimensions. A slowly oscillating field also induces a polarization $P_i = \chi_{ij}(0)E_j$. Its time derivative is the current, which explains the factor $-\mathrm{i}z$ and gives $\chi_{xx}(0)$ directly from the negative slope of $\mathrm{Im}\,\sigma_{xx}$. The quadratic Hall term weights curvature by the inverse squared gap. If time-reversal symmetry is broken, regions

of opposite curvature can cancel in the dc Hall conductivity and still produce Faraday rotation at finite frequency because their gaps differ. With time-reversal symmetry the partners cancel at each frequency.

At frequencies large compared with the transition energies retained in the model, expanding the same denominators in Δ_{mn}/z gives

$$\sigma_{ij}(z) = \frac{\mathrm{i}}{z}\underbrace{2e^2\int_{\mathbf{k}}\sum_{nm}{}' \Delta_{mn} g_{ij}^{nm}}_{\substack{K_{ij}=n_e e^2 (m_{\mathrm{opt}}^{-1})_{ij} \\ \text{optical weight coefficient}}} + \frac{1}{z^2}\underbrace{e^2\int_{\mathbf{k}}\sum_{nm}{}' \Delta_{mn}^2 \Omega_{ij}^{nm}}_{\substack{h_{ij}^{(-2)} \\ \text{high-frequency Hall moment}}} + O(z^{-3}). \tag{2.47}$$

The symmetric coefficient K_{ij} defines the inverse optical mass per electron. With the power of z indicated in the superscript of each Hall coefficient, the high-frequency expansion reads

$$\sigma_{ij}(z) = \frac{\mathrm{i}}{z} n_e e^2 (m_{\mathrm{opt}}^{-1})_{ij} + \frac{h_{ij}^{(-2)}}{z^2} + O(z^{-3}). \tag{2.48}$$

Thus $\omega \operatorname{Im}\sigma_{xx}(\omega)$ approaches K_{xx}, and the integrated longitudinal optical weight is $\pi K_{xx}/2$. For the complete continuum spectrum with a local potential, the f-sum rule gives $(m_{\mathrm{opt}}^{-1})_{ij} = \delta_{ij}/m_e$. A restricted band model has its own optical mass because it omits transitions to remote bands. In a metal the Drude coefficient D_{ij} must be added to the interband contribution to K_{ij}. The $1/z^2$ term is antisymmetric and weights curvature by the squared gap. In the continuum the high-frequency expansion requires the corresponding spectral moments to converge.

How do we recover these coefficients from an absorption experiment? For a real probe frequency ω away from the absorption spectrum, the positive-frequency Kramers–Kronig relations give

$$\begin{aligned} \operatorname{Im}\sigma_{xx}(\omega) &= -\frac{2\omega}{\pi}\int_0^\infty \frac{\operatorname{Re}\sigma_{xx}(\nu)}{\nu^2-\omega^2}\,\mathrm{d}\nu, \\ \operatorname{Re}\sigma_{xy}^A(\omega) &= \frac{2}{\pi}\int_0^\infty \frac{\nu \operatorname{Im}\sigma_{xy}^A(\nu)}{\nu^2-\omega^2}\,\mathrm{d}\nu. \end{aligned} \tag{2.49}$$

Below the gap the kernel begins with $1/\nu^2$. The longitudinal numerator supplies one power of the probe frequency ω, while the Hall numerator supplies one power of the transition frequency ν. Matching the longitudinal slope and the Hall intercept to Eq. (2.45) gives

$$\begin{aligned} \chi_{xx}(0) &= -\lim_{\omega\to 0}\frac{\operatorname{Im}\sigma_{xx}(\omega)}{\omega} = \frac{2}{\pi}\int_0^\infty \frac{\operatorname{Re}\sigma_{xx}(\nu)}{\nu^2}\,\mathrm{d}\nu = \frac{2}{\pi}\mathcal{S}_{L,x}^{-1}, \\ \sigma_{xy}^A(0) &= \lim_{\omega\to 0}\operatorname{Re}\sigma_{xy}^A(\omega) = \frac{2}{\pi}\int_0^\infty \frac{\operatorname{Im}\sigma_{xy}^A(\nu)}{\nu}\,\mathrm{d}\nu = -\frac{2}{\pi}\mathcal{S}_{H,z}^{0}. \end{aligned}$$

At the other end of the spectrum the kernel begins with $-1/\omega^2$, independent of the transition frequency. Now every absorption peak contributes its area. Matching the $1/\omega$ term to Eq. (2.47) gives

$$K_{xx} = n_e e^2 (m_{\mathrm{opt}}^{-1})_{xx} = \lim_{\omega\to\infty}\omega \operatorname{Im}\sigma_{xx}(\omega) = \frac{2}{\pi}\int_0^\infty \operatorname{Re}\sigma_{xx}(\nu)\,\mathrm{d}\nu = \frac{2}{\pi}\mathcal{S}_{L,x}^{1}.$$

The same matching identifies the two frequency-dependent Hall coefficients. Keeping the next term ω^2/ν^4 in the low-frequency kernel gives the quadratic Hall dispersion. Keeping $-1/\omega^2$ in the high-frequency kernel gives the leading Hall moment.

$$h_{xy}^{(2)} = \frac{1}{2}\left.\frac{\mathrm{d}^2 \operatorname{Re}\sigma_{xy}^A}{\mathrm{d}\omega^2}\right|_{\omega=0} = \frac{2}{\pi}\int_0^\infty \frac{\operatorname{Im}\sigma_{xy}^A(\nu)}{\nu^3}\,\mathrm{d}\nu = -\frac{2}{\pi}\mathcal{S}_{H,z}^{-2},$$
$$h_{xy}^{(-2)} = \lim_{\omega\to\infty}\omega^2 \operatorname{Re}\sigma_{xy}^A(\omega) = -\frac{2}{\pi}\int_0^\infty \nu\,\operatorname{Im}\sigma_{xy}^A(\nu)\,\mathrm{d}\nu = \frac{2}{\pi}\mathcal{S}_{H,z}^{2}.$$

The superscript on $\mathcal{S}$ labels the moment order. Table 1 collects the three orders $-1, 0, 1$. For example, the optical mass can be read from the high-frequency current or inferred by adding up the absorption over the same spectrum.

∴ **The optical Hall angle and Faraday rotation**

For an in-plane isotropic insulator the optical Hall ratio is $R_H = \sigma_{xy}^A/\sigma_{xx}$. A transmission experiment also sees the substrate. For light normally incident from vacuum on a sheet on a transparent semi-infinite substrate, the transmitted field satisfies $E_y/E_x = \sigma_{xy}^A/(Y+\sigma_{xx})$, where $Y = c(1+n_s)/(4\pi)$ in Gaussian units. For weak rotation and ellipticity, $\theta_F \simeq \operatorname{Re}(E_y/E_x)$. The leading terms for $|\sigma_{xx}| \ll Y$ follow from the sheet sum rules.

	Hall ratio R_H	Faraday angle θ_F
Below the gap ($\mathcal{S}_{H,z}^0 = 0$)	$-\mathrm{i}\omega\,\dfrac{\mathcal{S}_{H,z}^{-2}}{\mathcal{S}_{L,x}^{-1}}$	$-\dfrac{2\omega^2}{\pi Y}\,\mathcal{S}_{H,z}^{-2}$
Above the retained transitions	$-\dfrac{\mathrm{i}}{\omega}\,\dfrac{\mathcal{S}_{H,z}^{2}}{\mathcal{S}_{L,x}^{1}}$	$\dfrac{2}{\pi Y\omega^2}\,\mathcal{S}_{H,z}^{2}$

Below the gap the linear Hall slope compares curvature weighted by $1/\Delta^2$ with metric weighted by $1/\Delta$. The transmitted rotation starts quadratically because its denominator tends to Y. Both leading Hall ratios in the table are imaginary. The Faraday angle measures a real rotation, taken positive from $\hat{\mathbf{x}}$ toward $\hat{\mathbf{y}}$. A finite dc Hall term gives a Faraday intercept, $\tan\theta_F(0) = -2\mathcal{S}_{H,z}^0/(\pi Y)$ (Wu et al., 2016).

2.10 One absorption spectrum, several moments

Given this compact form of the conductivity, what are all the sum rules that we can write? For the longitudinal response of an insulator, define the moments of the absorption

$$\mathcal{S}_{L,x}^{\eta} = \int_0^\infty \omega^{\eta-1}\operatorname{Re}\sigma_{xx}(\omega)\,\mathrm{d}\omega = \pi e^2\int_{\mathrm{BZ}}\frac{\mathrm{d}^d k}{(2\pi)^d}\sum_{\substack{n\in\mathrm{occ}\\ m\in\mathrm{emp}}}\Delta_{mn}^{\eta} g_{xx}^{nm}. \tag{2.50}$$

The same transitions can be measured with circularly polarized light. Half the difference between the two absorptions is $(A_+ - A_-)/2 = -\operatorname{Im}\sigma_{xy}^A$ in our convention. With z here denoting the axis normal to the xy plane in the Hall subscript, its moment is

$$\mathcal{S}_{H,z}^{\eta} = -\int_0^\infty \omega^{\eta-1}\operatorname{Im}\sigma_{xy}^A(\omega)\,\mathrm{d}\omega = \frac{\pi e^2}{2}\int_{\mathrm{BZ}}\frac{\mathrm{d}^d k}{(2\pi)^d}\sum_{\substack{n\in\mathrm{occ}\\ m\in\mathrm{emp}}}\Delta_{mn}^{\eta}\Omega_{xy}^{nm}. \tag{2.51}$$

The longitudinal spectrum is positive, while the Hall spectrum can change sign because either handedness can absorb more strongly. For a monochromatic field the cycle-averaged power density is $\frac{1}{2}\,\mathrm{Re}(\mathbf{E}^\dagger\sigma\mathbf{E})$. Only the Hermitian part of σ enters this power. For the longitudinal response this picks out $\mathrm{Re}\,\sigma_{xx}$, while for the antisymmetric transverse response it picks out $\mathrm{Im}\,\sigma^A_{xy}$. This is why a Hall current can flow without dissipation at zero frequency even though the Hall spectrum at optical frequencies can show absorption.

The same hierarchy appears directly in time. Each time derivative of $\mathcal{Q}_{xx}(t)$ in Eq. (2.19) brings down one factor of the transition energy, so for a nonnegative integer η

$$\mathcal{S}^{\eta}_{L,x} = \pi e^2[(\mathrm{i}\partial_t)^\eta \mathcal{Q}_{xx}(t)]_{t=0}. \tag{2.52}$$

All of these sum rules are therefore time derivatives of the polarization fluctuation, evaluated at $t = 0$. For negative powers the inverse derivative has to be defined on the spectrum, $(\mathrm{i}\partial_t)^{-1}e^{-\mathrm{i}\Delta t} = e^{-\mathrm{i}\Delta t}/\Delta$ for $\Delta > 0$, because an integral from 0 to t would vanish at $t = 0$, and here the gap and the convergence of the moment matter.

Optical sum rules in a gapped insulator

	Longitudinal	**Transverse (Hall)**
Absorptive	$\mathrm{Re}\,\sigma_{xx}$	$\mathrm{Im}\,\sigma^A_{xy}$
Nondissipative	$\mathrm{Im}\,\sigma_{xx}$	$\mathrm{Re}\,\sigma^A_{xy}$
Weight	*Moment of* $\mathrm{Re}\,\sigma_{xx}$	*Moment of* $-\mathrm{Im}\,\sigma^A_{xy}$
$\eta = -1$ $\frac{\mathrm{d}\omega}{\omega^2}$	**Static polarizability** $\mathcal{S}^{-1}_{L,x} = \frac{\pi}{2}\chi_{xx}(0)$ Read $\chi_{xx}(0)$ from the negative slope of $\mathrm{Im}\,\sigma_{xx}$ below the gap.	**Low-energy dichroism** $\mathcal{S}^{-1}_{H,z} = \frac{\pi e^2}{2}\int_{\mathrm{BZ}}\frac{\mathrm{d}^d k}{(2\pi)^d}\sum_{\substack{n\in\mathrm{occ}\\ m\in\mathrm{emp}}}\frac{\Omega^{nm}_{xy}}{\Delta_{mn}}$ Low-energy transitions contribute most strongly for a given curvature.
$\eta = 0$ $\frac{\mathrm{d}\omega}{\omega}$	**Localization tensor** $\mathcal{S}^{0}_{L,x} = \pi e^2\mathcal{Q}_{xx}(0)$ Per electron the position variance is $\ell_x^2 = \mathcal{Q}_{xx}(0)/n_e$.	**dc Hall conductivity** $\mathcal{S}^{0}_{H,z} = -\frac{\pi}{2}\sigma^A_{xy}(0)$ Read $\sigma^A_{xy}(0)$ from the zero-frequency intercept of $\mathrm{Re}\,\sigma^A_{xy}$.
$\eta = 1$ $\mathrm{d}\omega$	**Optical weight** $\mathcal{S}^{1}_{L,x} = \frac{\pi}{2}K_{xx}$ Read K_{xx} from the $1/\omega$ tail of $\mathrm{Im}\,\sigma_{xx}$. For the full continuum, $K_{xx} = n_e e^2/m_e$.	**Orbital circulation** $\mathcal{S}^{1}_{H,z} = \frac{\pi e^2}{2}\int_{\mathrm{BZ}}\frac{\mathrm{d}^d k}{(2\pi)^d}\sum_{\substack{n\in\mathrm{occ}\\ m\in\mathrm{emp}}}\Delta_{mn}\Omega^{nm}_{xy}$ The dichroic f-sum measures the gauge-invariant part of Wannier self-rotation.

Table 1: The shaded cells can also be measured from the nondissipative conductivity in Eqs. (2.45) and (2.47). Read down either column to change the frequency weight applied to the same absorption measurement (Verma and Queiroz, 2025a). The localization and orbital-circulation sums are due to Souza et al. (2000) and Souza and Vanderbilt (2008), respectively.

The $\eta = -1$ Hall moment has a more tentative interpretation. It measures low-energy circular dichroism, and whether it can be identified with an electronic torsional response remains open.

2.11 A useful bound and the single-frequency limit

The longitudinal moments obey a family of inequalities (Verma and Queiroz, 2025a). Because absorption is positive, $\mathrm{d}\mu = \mathrm{Re}\,\sigma_{xx}(\omega)\mathrm{d}\omega/\omega$ is a nonnegative measure, and the Cauchy–Schwarz inequality applied to the functions 1 and ω gives

$$(\mathcal{S}^1_{L,x})^2 \le \mathcal{S}^0_{L,x}\mathcal{S}^2_{L,x}. \tag{2.53}$$

Applied to $\omega^{-1/2}$ and $\omega^{1/2}$, it gives

$$(\mathcal{S}^0_{L,x})^2 \le \mathcal{S}^{-1}_{L,x}\mathcal{S}^1_{L,x}. \tag{2.54}$$

If all the optical transitions happen at one frequency ω_0, then $\mathcal{S}^\eta_{L,x} = \omega_0^\eta \mathcal{S}^0_{L,x}$ and both bounds are saturated. This is the case of the lowest Landau level, and it is why the quantum Hall problem is so beautiful: with a single frequency, all of these quantities are fixed by the magnetic length and by powers of ω_c. A crystal with several active transition energies gives strict inequalities, and the excess measures how spread out its optical frequencies are.

∴ **One filled Landau level: the full response and every moment**

Let $s = \mathrm{sgn}\,\Omega_{xy}$ specify the orientation. Per occupied orbital,

$$\mathcal{G} = \frac{\ell_B^2}{2}\begin{pmatrix} 1 & -\mathrm{i}s \\ \mathrm{i}s & 1 \end{pmatrix}, \qquad \Delta = \omega_c, \qquad n_{\mathrm{LL}} = \frac{1}{2\pi\ell_B^2}. \tag{2.55}$$

With one spin species and one filled level, multiplying by the degeneracy per area gives

$$\mathcal{Q}(t) = \frac{e^{-\mathrm{i}\omega_c t}}{4\pi}\begin{pmatrix} 1 & -\mathrm{i}s \\ \mathrm{i}s & 1 \end{pmatrix}. \tag{2.56}$$

Insert this single transition into the longitudinal and transverse response formulas. Combining the positive- and negative-frequency poles yields

$$\sigma_{xx}(z) = \frac{\mathrm{i}e^2}{2\pi}\frac{\omega_c z}{z^2-\omega_c^2}, \tag{2.57}$$

$$\sigma_{xy}(z) = \frac{se^2}{2\pi}\frac{\omega_c^2}{z^2-\omega_c^2}. \tag{2.58}$$

The same retarded variable $z = \omega + \mathrm{i}0^+$ occurs in both factors of the denominator. At positive frequency,

$$\mathrm{Re}\,\sigma_{xx}(\omega) = \frac{e^2\omega_c}{4}\delta(\omega-\omega_c), \qquad \mathrm{Im}\,\sigma_{xy}(\omega) = -\frac{se^2\omega_c}{4}\delta(\omega-\omega_c). \tag{2.59}$$

The moments of Eq. (2.50) follow:

$$\sigma_{xy}(0) = -\frac{se^2}{2\pi}, \qquad \mathcal{S}^\eta_{L,x} = \frac{e^2}{4}\omega_c^\eta, \qquad \chi_{xx}(0) = \frac{e^2}{2\pi\omega_c}. \tag{2.60}$$

The f-sum is $\mathcal{S}^1_{L,x} = e^2\omega_c/4 = \pi n_{\mathrm{LL}}e^2/(2m_e)$ because $\omega_c\ell_B^2 = 1/m_e$, so the Landau level exhausts the optical weight of free electrons with a single transition, and every other moment follows by multiplying by another power of ω_c. One has to be careful with the normalization when comparing a length in the wave function with a measured response: the susceptibility per orbital is $e^2\ell_B^2/\omega_c \propto |B|^{-2}$, while the susceptibility per area above scales as $|B|^{-1}$, because the number of occupied orbitals grows with the field.

∴ **The excess in a sum-rule bound is a spectral width**

Assume $\mathcal{S}^0_{L,x} > 0$ and the required moments converge. Normalize the positive optical measure to a probability distribution,

$$\mathrm{d}p(\omega) = \frac{\operatorname{Re}\sigma_{xx}(\omega)}{\mathcal{S}^0_{L,x}\,\omega}\,\mathrm{d}\omega, \qquad \int \mathrm{d}p = 1. \tag{2.61}$$

Its mean and variance follow without fitting a resonance:

$$\langle\omega\rangle_p = \frac{\mathcal{S}^1_{L,x}}{\mathcal{S}^0_{L,x}}, \qquad \mathrm{Var}_p(\omega) = \frac{\mathcal{S}^0_{L,x}\mathcal{S}^2_{L,x} - (\mathcal{S}^1_{L,x})^2}{(\mathcal{S}^0_{L,x})^2}. \tag{2.62}$$

The excess in the first Cauchy–Schwarz bound is therefore the variance of the optical frequencies, and the same variance controls how quickly the fluctuation loses coherence in time. Since

$$\frac{\mathcal{Q}_{xx}(t)}{\mathcal{Q}_{xx}(0)} = \int e^{-\mathrm{i}\omega t}\,\mathrm{d}p(\omega), \tag{2.63}$$

expansion at $t = 0$ gives

$$\left|\frac{\mathcal{Q}_{xx}(t)}{\mathcal{Q}_{xx}(0)}\right|^2 = 1 - \mathrm{Var}_p(\omega)t^2 + o(t^2). \tag{2.64}$$

A single frequency only changes the phase of the correlator. A spread of frequencies reduces its modulus, which is dephasing without any scattering.
The inverse-moment bound has an equally explicit two-line check. For $\mathrm{d}\mu = w_1\delta(\omega - \Delta_1)\mathrm{d}\omega + w_2\delta(\omega - \Delta_2)\mathrm{d}\omega$, with $w_i > 0$ and $\Delta_i > 0$, multiplication gives

$$\mathcal{S}^0_{L,x}\mathcal{S}^2_{L,x} - (\mathcal{S}^1_{L,x})^2 = w_1 w_2(\Delta_1 - \Delta_2)^2, \tag{2.65}$$

$$\mathcal{S}^{-1}_{L,x}\mathcal{S}^1_{L,x} - (\mathcal{S}^0_{L,x})^2 = w_1 w_2\frac{(\Delta_1 - \Delta_2)^2}{\Delta_1\Delta_2}. \tag{2.66}$$

Both vanish only when the two active frequencies coincide. The second excess weights their separation relative to their energies.

3 Lecture 3: Optical weight, bonding and lattice interference

3.1 Deriving the f-sum rule

The continuum optical f-sum is the conductivity form of the Thomas–Reiche–Kuhn oscillator-strength rule (Reiche and Thomas, 1925; Kuhn, 1925). In the first lecture we said that a lattice does not change the total optical weight of electrons in the continuum, it only redistributes it. In the second we found that each interband transition contributes its energy times its metric, $\Delta_{mn} g_{xx}^{nm}$. Let us connect the two statements and see what is geometric and what is not in the f-sum rule. What is special about this sum rule, and not true of the others, is that it does not depend on the material. If we do not restrict ourselves to low-energy bands, the Hamiltonian of any solid is a kinetic energy plus a potential that depends only on position, which contains the lattice and everything else.

For the Bloch Hamiltonian $H(\mathbf{k}) = (\mathbf{p} + \mathbf{k})^2/(2m_e) + V(\mathbf{r})$, taking two derivatives with respect to momentum leaves only a constant,

$$\partial_{k_x}^2 H = \frac{1}{m_e}. \tag{3.1}$$

The mass that appears is the bare mass of the electron, because the potential has dropped out. The whole f-sum rule comes down to this constant and to how many electrons we have. To see how the constant is shared, we differentiate the spectral decomposition $H = \sum_l \varepsilon_l P_l$ twice and take the expectation value in the state $|u_n\rangle$:

$$\langle u_n | \partial_x^2 H | u_n \rangle = \partial_x^2 \varepsilon_n + \sum_l \varepsilon_l \langle u_n | \partial_x^2 P_l | u_n \rangle. \tag{3.2}$$

The product rule gives three terms, of which two survive in the display. The first is the curvature of the band, its inverse band mass. The cross term $2(\partial_x \varepsilon_l)\langle u_n | \partial_x P_l | u_n \rangle$ vanishes, because the derivative of a projector has no diagonal elements in the band basis, as we learned in Lecture 1. The last term contains the second derivative of the projectors, and since $\sum_l \partial_x^2 P_l = 0$ we can subtract ε_n from each of its coefficients, so that only energy differences appear.

∴ The inverse-mass identity

For $m \neq n$, expand $\partial_x^2 P_m = \partial_x^2(|u_m\rangle\langle u_m|)$. Orthogonality removes the terms with an undifferentiated $|u_m\rangle$ or $\langle u_m|$. The middle term gives

$$\langle u_n | \partial_x^2 P_m | u_n \rangle = 2 |\langle u_n | \partial_x u_m \rangle|^2 = 2 g_{xx}^{nm}. \tag{3.3}$$

Hence

$$\boxed{\frac{1}{m_e} = \partial_x^2 \varepsilon_n + 2 \sum_{m \neq n} \Delta_{mn} g_{xx}^{nm}.} \tag{3.4}$$

This is the effective-mass identity familiar from $\mathbf{k} \cdot \mathbf{p}$ theory. The curvature of one band gives its inverse effective mass along x. The interband terms account for the difference between that curvature and the inverse bare mass. Now sum over the occupied n and integrate over momentum. The terms between two occupied bands cancel in pairs because $\Delta_{mn} = -\Delta_{nm}$ and $g_{xx}^{nm} = g_{xx}^{mn}$, and using Eq. (2.44),

$$\frac{n_e e^2}{m_e} = D_{xx} + 2e^2 \int_{\mathrm{BZ}} \frac{\mathrm{d}^d k}{(2\pi)^d} \sum_{\substack{n \in \mathrm{occ} \\ m \in \mathrm{emp}}} \Delta_{mn} g_{xx}^{nm}. \tag{3.5}$$

Multiplication by $\pi/2$ gives

$$\boxed{\frac{\pi D_{xx}}{2} + \int_{0^+}^{\infty} \mathrm{Re}\,\sigma_{xx}^{\mathrm{inter}}(\omega)\,\mathrm{d}\omega = \frac{\pi n_e e^2}{2m_e}.} \tag{3.6}$$

The lower limit 0^+ separates the interband absorption from the delta function at zero frequency, of which only half lies on the positive axis, hence the factor 1/2 on the Drude term.

The three terms have a simple reading. The right-hand side counts all the charge that we have. The Drude weight is whatever lives on the Fermi surface, and the interband integral is the weight that the lattice has moved to finite frequency. Dividing by the total, one can write $n_e = n_{\mathrm{itinerant}} + n_{\mathrm{bound}}$, both with the bare mass: looking at the conductivity gives a natural way to separate the part of the charge that moves from the part that is bound, which oscillates around its position and whose weight records how the wave functions change with momentum. One should keep in mind that these are the same electrons responding in two ways, and that such an optical "itinerant fraction" is a division of oscillator strength over a specified range of frequencies.

In a lattice model truncated to a few bands the second derivative of the Hamiltonian is no longer a constant. We then replace $1/m_e$ in Eq. (3.4) by $\langle u_n|\partial_x^2 H|u_n\rangle$, with the electromagnetic coupling implemented consistently, and the restricted sum is

$$\int_0^{\infty} \mathrm{Re}\,\sigma_{xx}^{\mathrm{model}}(\omega)\,\mathrm{d}\omega = \frac{\pi e^2}{2}\int_{\mathrm{BZ}} \frac{\mathrm{d}^d k}{(2\pi)^d} \sum_n f_n \langle u_n|\partial_x^2 H|u_n\rangle. \tag{3.7}$$

This restricted sum is not universal: it changes when we change the hopping parameters, even in a two-band model. The transitions to the high-energy states that the model left out restore the complete sum of the continuum.

∴ Where the geometric diamagnetic weight goes

We can now go back to the standard derivation and see how it contains the same result. Minimal coupling gives two terms in the current response, $\sigma_{xx}(z) = (\mathrm{i}/z)[K_{xx} + \chi_{xx}^{jj}(z)]$ (Appendix A.3). The diamagnetic term is

$$K_{xx} = e^2 \int_{\mathrm{BZ}} \frac{\mathrm{d}^d k}{(2\pi)^d} \sum_n f_n \langle u_n|\partial_x^2 H|u_n\rangle. \tag{3.8}$$

The steps leading to Eq. (3.4) never used the form of $\partial_x^2 H$. In general,

$$\langle u_n|\partial_x^2 H|u_n\rangle = \partial_x^2 \varepsilon_n + 2\sum_{m\neq n} \Delta_{mn} g_{xx}^{nm}, \tag{3.9}$$

and summing over occupied states, where occupied-to-occupied terms cancel in pairs,

$$K_{xx} = D_{xx} + 2e^2 \int_{\mathrm{BZ}} \frac{\mathrm{d}^d k}{(2\pi)^d} \sum_{\substack{n\in\mathrm{occ} \\ m\in\mathrm{emp}}} \Delta_{mn} g_{xx}^{nm}. \tag{3.10}$$

Now use $|v_x^{nm}|^2 = \Delta_{mn}^2 g_{xx}^{nm}$ in the retarded current correlator. Combining the two orderings of each transition gives

$$\chi_{xx}^{jj}(z) = e^2 \int_{\mathrm{BZ}} \frac{\mathrm{d}^d k}{(2\pi)^d} \sum_{\substack{n\in\mathrm{occ} \\ m\in\mathrm{emp}}} \Delta_{mn}^2 g_{xx}^{nm} \left[\frac{1}{z-\Delta_{mn}} - \frac{1}{z+\Delta_{mn}}\right] \tag{3.11}$$

$$= 2e^2 \int_{\mathrm{BZ}} \frac{\mathrm{d}^d k}{(2\pi)^d} \sum_{\substack{n\in\mathrm{occ} \\ m\in\mathrm{emp}}} \frac{\Delta_{mn}^3 g_{xx}^{nm}}{z^2-\Delta_{mn}^2}. \tag{3.12}$$

At $z = 0$ this is precisely minus the geometric term in K_{xx}. At finite z, combine the fractions before dividing by z:

$$K_{xx} + \chi_{xx}^{jj}(z) = D_{xx} + 2e^2 \int_{\mathrm{BZ}} \frac{\mathrm{d}^d k}{(2\pi)^d} \sum_{\substack{n\in\mathrm{occ} \\ m\in\mathrm{emp}}} \frac{z^2 \Delta_{mn} g_{xx}^{nm}}{z^2-\Delta_{mn}^2}, \tag{3.13}$$

$$\sigma_{xx}(z) = \frac{\mathrm{i}D_{xx}}{z} + 2\mathrm{i}e^2 z \int_{\mathrm{BZ}} \frac{\mathrm{d}^d k}{(2\pi)^d} \sum_{\substack{n\in\mathrm{occ} \\ m\in\mathrm{emp}}} \frac{\Delta_{mn} g_{xx}^{nm}}{z^2-\Delta_{mn}^2}. \tag{3.14}$$

This is the conductivity that we obtained in Lecture 2 from the dipole response. The diamagnetic term contains a geometric piece that the paramagnetic correlator cancels exactly at zero frequency, so the interband $1/z$ pole disappears and what is left is the geometric response at finite frequency. In an insulator $D_{xx} = 0$ by periodicity, and in a clean metal the pole that remains is the Drude term. The static argument, pair by pair, assumes nonzero transition gaps and convergent sums; a gapless interband limit must be taken in the full frequency-dependent expression.

3.2 Energy gaps do not determine polarization

The usual estimate of the dielectric constant of a semiconductor is that it goes as the inverse of the gap. Equation (2.27) shows what this estimate misses: the susceptibility contains an energy denominator and a dipole matrix element. A large gap suppresses the polarization, but it does not fix it, because two systems with the same transition energies can have very different matrix elements.

The simplest example that separates the two ingredients is a single bond. Put two sites at $x = \pm a/2$, keep one orbital on each, and occupy the lower eigenstate of

$$H = \delta\sigma_z + t_h\sigma_x, \qquad x = \frac{a}{2}\sigma_z, \qquad E = \sqrt{\delta^2 + t_h^2}, \quad \Delta = 2E. \tag{3.15}$$

The onsite imbalance δ wants the electron on one site, and the hopping t_h wants to share it between the two. In the lower state $\langle x\rangle = -a\delta/(2E)$ and $\langle x^2\rangle = a^2/4$, so the fluctuation of position is

$$g = \langle x^2\rangle - \langle x\rangle^2 = \frac{a^2 t_h^2}{4E^2} = |\langle -|x|+\rangle|^2. \tag{3.16}$$

Writing $t_h = E\sin\theta$ and $\delta = E\cos\theta$ lets us vary the fluctuation at fixed gap. Per bond, the variance, static polarizability and correlator are

$$g = \frac{a^2}{4}\sin^2\theta, \qquad \chi_{xx}(0) = \frac{2e^2 g}{\Delta}, \qquad \mathcal{Q}_{xx}(t) = g e^{-\mathrm{i}\Delta t}. \tag{3.17}$$

At $\theta = 0$ the electron sits on one site, the bond is completely ionic and the dipole fluctuation vanishes. At $\theta = \pi/2$ the electron is shared equally between the two sites, the bond is covalent and the variance is $a^2/4$. The gap is the same in both cases. What changed is where the electron is, and a field that pokes one site of a covalent bond necessarily moves charge on the other. In this model the sites are points; the fluctuations inside each atomic orbital would add further transitions at higher energy.

3.3 From an isolated bond to a chain

The same choice appears in a crystal. Take a chain with one orbital per site at half filling. It does not want to stay a metal, and it can open a gap in two ways. It can make the two sites of a doubled cell different in energy, so that the electrons sit on one of them, as in an ionic compound. Or it can make the bonds alternate in strength, so that the electrons sit in the middle of the strong bonds, which is what the hybridization between orbitals does in a covalent semiconductor. The Rice–Mele model includes both possibilities (Rice and Mele, 1982). With a cell of period a, orbitals at positions 0 and $a/2$, hoppings v and w and an onsite imbalance δ, the Bloch Hamiltonian with the positions of the orbitals included is

$$H(k) = \begin{pmatrix} \delta & ve^{\mathrm{i}ka/2} + we^{-\mathrm{i}ka/2} \\ ve^{-\mathrm{i}ka/2} + we^{\mathrm{i}ka/2} & -\delta \end{pmatrix} = \mathbf{d}(k) \cdot \boldsymbol{\sigma}, \tag{3.18}$$

where $\mathbf{d} = ((v+w)\cos(ka/2), -(v-w)\sin(ka/2), \delta)$. The two energies are $\pm|\mathbf{d}|$, and for the lower band the projector $P_- = (1 - \hat{\mathbf{d}} \cdot \boldsymbol{\sigma})/2$ gives

$$g_{kk} = \frac{1}{4} \partial_k \hat{\mathbf{d}} \cdot \partial_k \hat{\mathbf{d}}. \tag{3.19}$$

It is a good exercise to derive this directly from Eq. (1.15), where the Pauli identity $\mathrm{Tr}(\sigma_i \sigma_j) = 2\delta_{ij}$ supplies the factor $1/4$.

Two limits are easy to understand. When $w = 0$ and $\delta = 0$ the chain is a collection of isolated bonds of length $a/2$, and the metric is $a^2/16$, exactly the position variance of each bond. When $v = w$ and $\delta = 0$ we are back to the uniform chain, the two folded bands touch and the chain is a metal. The metric grows without limit as we approach this point from the gapped side, in agreement with what we said about metals in Lecture 1, and at the touching point the projector onto one band is not defined.

The physical positions of the orbitals matter in all of this. If we change to a basis in which the Hamiltonian is periodic in momentum, the information about the positions moves from $H(k)$ into the position operator, and the physical response then requires both the derivative of the transformed Hamiltonian and the connection that appears in the position operator.

∴ The integrated metric of the dimerized chain, exactly

Set the onsite imbalance to zero in the embedded chain above and take $v, w > 0$, $v \neq w$. Keep the orbital positions at 0 and $a/2$. Write

$$A = v + w, \quad B = v - w, \quad q = ka, \qquad \mathbf{d} = (A\cos(q/2), -B\sin(q/2), 0). \tag{3.20}$$

For any nonzero $\mathbf{d}$, $|\partial_k \hat{\mathbf{d}}|^2 = |\mathbf{d} \times \partial_k \mathbf{d}|^2 / |\mathbf{d}|^4$. Here

$$(\mathbf{d} \times \partial_k \mathbf{d})_z = -\frac{aAB}{2}, \qquad |\mathbf{d}|^2 = v^2 + w^2 + 2vw\cos q. \tag{3.21}$$

Consequently,

$$g_{kk}(k) = \frac{a^2(v^2 - w^2)^2}{16(v^2 + w^2 + 2vw\cos ka)^2}. \tag{3.22}$$

Define the per-cell Brillouin-zone average $\bar{g} = (a/2\pi)\int_{-\pi/a}^{\pi/a} g_{kk}(k)\,\mathrm{d}k$. For $c > |b|$, the substitution $u = \tan(q/2)$ gives

$$\frac{1}{2\pi}\int_{-\pi}^{\pi} \frac{\mathrm{d}q}{c + b\cos q} = \frac{1}{\pi}\int_{-\infty}^{\infty} \frac{\mathrm{d}u}{(c+b) + (c-b)u^2} = \frac{1}{\sqrt{c^2 - b^2}}. \tag{3.23}$$

Differentiate with respect to c at fixed b:

$$\frac{1}{2\pi}\int_{-\pi}^{\pi} \frac{\mathrm{d}q}{(c + b\cos q)^2} = \frac{c}{(c^2 - b^2)^{3/2}}. \tag{3.24}$$

With $c = v^2 + w^2$ and $b = 2vw$, this yields

$$\boxed{\bar{g} = \frac{a^2}{16}\frac{v^2 + w^2}{|v^2 - w^2|}.} \tag{3.25}$$

Either isolated-dimer limit gives $a^2/16$. As v approaches w, the zone-edge value diverges quadratically,

$$g_{kk}(\pi/a) = \frac{a^2(v+w)^2}{16(v-w)^2}, \qquad \bar{g} \sim \frac{a^2 w}{16|v-w|}. \tag{3.26}$$

The integral loses one inverse power because the peak narrows. At exactly $v = w$ the bands touch and the isolated-band projector is undefined at the touching point. To obtain the insulating limit, integrate first and then approach $v = w$ from the gapped side.

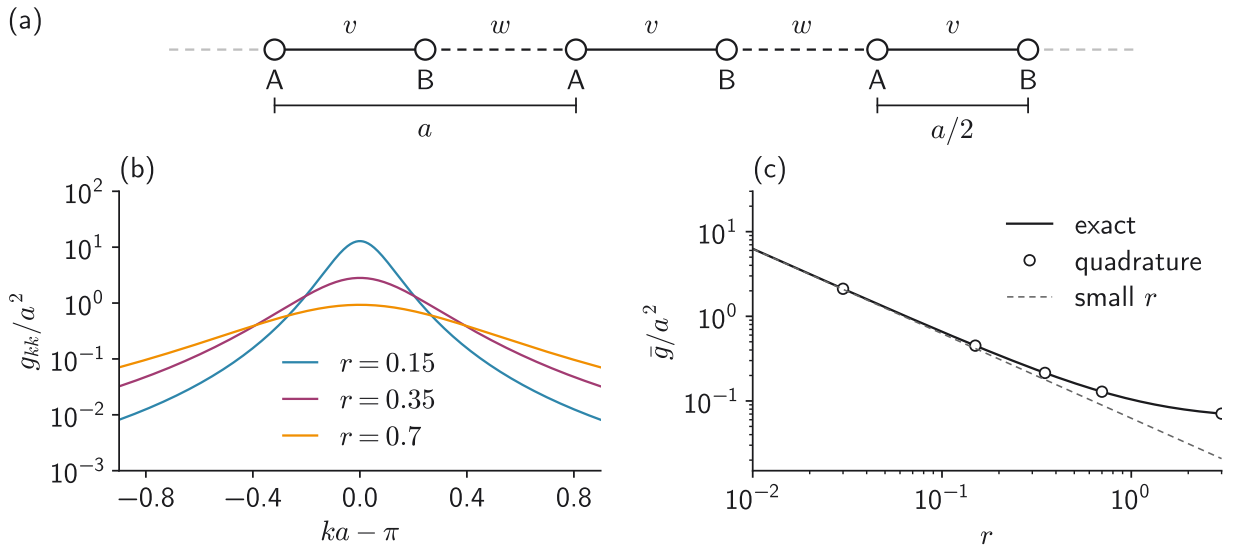


Figure 7: The physical orbital positions are 0 and $a/2$ in a cell of length a. The onsite imbalance is zero and $r = (v - w)/w > 0$. As r decreases, the metric peak at $q = ka = \pi$ grows and narrows. The Brillouin-zone average follows the exact result in the box, $\bar{g}/a^2 = [(1 + r)^2 + 1]/\{16[(1 + r)^2 - 1]\}$; the dashed curve is its small-r limit $1/(16r)$. The zone-edge peak diverges as r^{-2}, but its narrowing leaves an integrated r^{-1} divergence.

∴ How an ionic gap cuts off the chain divergence

Keep the same orbital embedding, set $v = w = t_h > 0$, and turn on onsite imbalance $\delta \neq 0$. Then

$$\mathbf{d} = (2t_h \cos(q/2), 0, \delta), \qquad q = ka. \tag{3.27}$$

From $g_{kk} = |\mathbf{d} \times \partial_k \mathbf{d}|^2/(4|\mathbf{d}|^4)$,

$$g_{kk}(q) = \frac{a^2 t_h^2 \delta^2 \sin^2(q/2)}{4[\delta^2 + 4t_h^2 \cos^2(q/2)]^2}. \tag{3.28}$$

Use the integral in the previous box with $c = \delta^2 + 2t_h^2$, $b = 2t_h^2$ and $R = \sqrt{c^2 - b^2}$. Differentiation with respect to c and b gives, with $\langle \cdot \rangle_q = (2\pi)^{-1} \int_{-\pi}^{\pi} \mathrm{d}q$,

$$\left\langle \frac{\sin^2(q/2)}{(c + b\cos q)^2} \right\rangle_q = \frac{1}{2}\left(\frac{c}{R^3} + \frac{b}{R^3}\right). \tag{3.29}$$

Therefore the full Brillouin-zone integral is

$$\boxed{\bar{g} = \frac{a^2 t_h^2}{8|\delta|\sqrt{\delta^2 + 4t_h^2}}.} \tag{3.30}$$

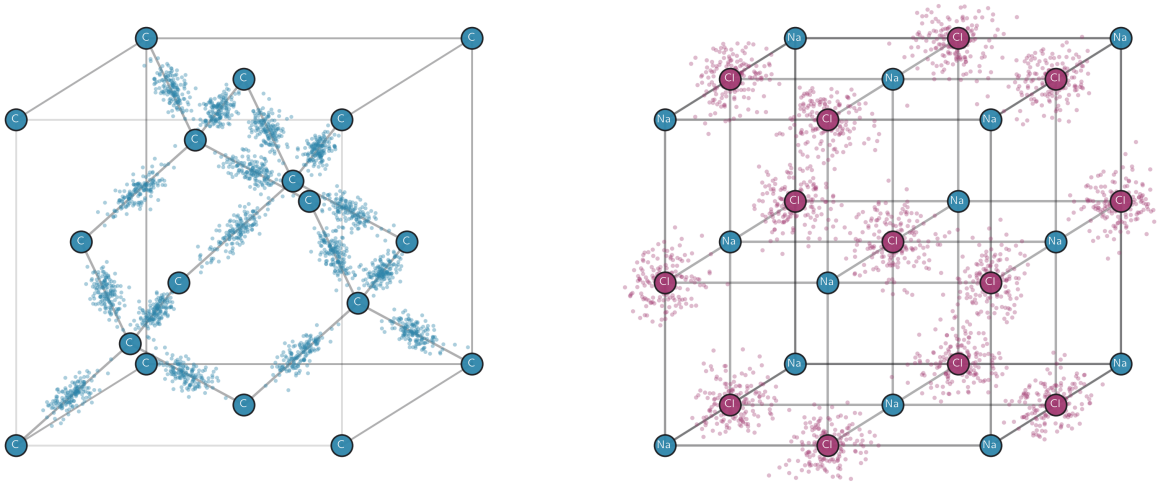
For $|\delta| \ll t_h$, this becomes $a^2 t_h/(16|\delta|)$. The metric at the zone edge is $a^2 t_h^2/(4\delta^2)$: its height diverges as $|\delta|^{-2}$ and its width in q is of order $|\delta|/t_h$. Their product explains the integrated $|\delta|^{-1}$ divergence. Deep in the ionic regime, $\bar{g} \sim a^2 t_h^2/(8\delta^2)$ and the state becomes localized on one sublattice. The same exact expression connects the narrow-gap enhancement to the atomic limit.

3.4 Bonding and the location of charge

This is the difference between ionic and covalent bonding in real materials. In an ionic crystal such as NaCl the occupied valence orbitals are centered near the anions. In diamond or silicon the occupied orbitals are bonding combinations of the hybridized orbitals of two neighboring atoms, and their Wannier functions are centered in the middle of the bonds. If we poke one atom of a covalent crystal, the orbital on that atom is shared between the bonding band, which is filled, and the antibonding band, which is empty, and this is what gives large position matrix elements between the two bands and a large metric.

A bond-centered orbital can therefore have large position fluctuations even in an insulator with a wide gap. Diamond combines a wide gap with a substantial refractive index. Its covalent bonds give valence electrons room to polarize along a bond, just as in the two-site example Komissarov et al. (2024). This is the reason to look at the wave functions, and not only at the gaps, when comparing dielectric responses. A quantitative comparison still requires the electron density, the distribution of transition energies and all the relevant dipole matrix elements.

Figure 8 shows the distinction in real space: the bonding charge can sit between the ions or near one species of ion. To calculate the response, this real-space picture has to be resolved into dipole matrix elements between occupied and empty states.



(a) Diamond: bond-centered charge (b) NaCl: anion-centered charge

Figure 8: Where the bonding charge sits (schematic). In diamond the cloud lies along the carbon–carbon bonds; in NaCl it sits near the chlorine sites.

There is a topological way of saying the same thing. When symmetry forces the Wannier centers of the occupied bands to sit away from the ionic sites, as in the middle of a bond, the insulator is called an obstructed atomic limit (Bradlyn et al., 2017). It has localized Wannier functions and zero Chern number, but there is nothing we can do, while keeping the symmetry, to move its electrons onto the atoms without closing the gap, and its optical response keeps the spatial structure of the bonds. A surface termination that cuts through these bond centers can leave dangling bonds. Whether

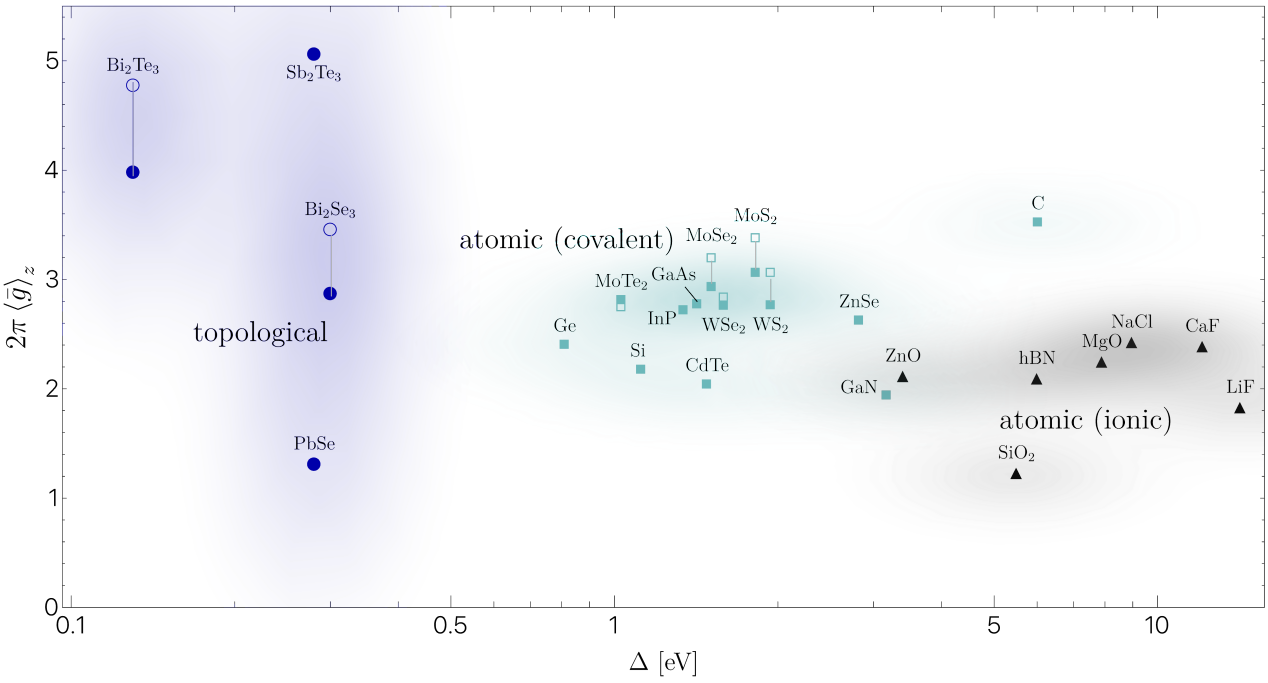


Figure 9: Material comparison from Komissarov et al. (2024). The vertical axis is $2\pi\langle\bar{g}\rangle_z$, a normalized geometric quantity estimated from the dielectric response and a characteristic gap; it is not the isolated-dimer variance g of Eq. (3.16). Filled symbols are estimates from experimental data and open symbols are fitted tight-binding calculations. Materials with similar gaps separate by bonding type.

they appear at a particular surface depends on where the crystal is cut and how the exposed atoms rearrange or bind to their surroundings.

How large is the fluctuation in a given material? We can estimate it from measurable quantities if we replace the full spectrum by a single characteristic optical energy ω_0, placed where most of the optical transitions happen. Writing $\mathcal{S}^1_{L,x} = \int_0^\infty \mathrm{Re}\,\sigma_{xx}(\omega)\,\mathrm{d}\omega$ for the longitudinal optical weight, this approximation gives

$$\chi_{xx}(0) \simeq \frac{2e^2\mathcal{Q}_{xx}(0)}{\omega_0}, \qquad \mathcal{S}^1_{L,x} \simeq \pi e^2\omega_0\mathcal{Q}_{xx}(0). \tag{3.31}$$

Eliminating the metric gives $\chi_{xx}(0) \simeq 2\mathcal{S}^1_{L,x}/(\pi\omega_0^2)$, an estimate of the Penn type (Penn, 1962). All of the bound charge is pictured as oscillating at the resonance frequency, with an amplitude set by the metric. The energy ω_0 represents the optically active part of the spectrum, and it can differ from both the smallest direct gap and the indirect fundamental gap. Figure 9 collects such estimates for many insulators. The general trend is that the fluctuation decreases as the gap increases, but materials with similar gaps separate systematically according to their bonding: covalent insulators such as diamond and silicon lie above ionic ones with a similar gap, and topological insulators lie higher still.

∴ **A geometric-length bound from two optical measurements**

The strong upper bound on localization relates the spread to the static electronic susceptibility and the total optical weight (Verma and Queiroz, 2025a; Onishi and Fu, 2025; Souza et al., 2025). For a three-dimensional bulk insulator in Gaussian units, let $\epsilon_{\infty,xx}$ be the static electronic dielectric response with the ions held fixed. Include the same complete electronic spectrum in both optical moments. With $\omega_p^2 = 4\pi n_e e^2/m_e$ and no Drude weight,

$$\mathcal{S}^1_{L,x} = \frac{\omega_p^2}{8}, \qquad \mathcal{S}^{-1}_{L,x} = \frac{\pi\chi_{xx}(0)}{2} = \frac{\epsilon_{\infty,xx}-1}{8}, \qquad \mathcal{S}^0_{L,x} = \pi e^2 \mathcal{Q}_{xx}(0). \tag{3.32}$$

Insert these three identities into $(\mathcal{S}^0_{L,x})^2 \le \mathcal{S}^{-1}_{L,x}\mathcal{S}^1_{L,x}$:

$$\boxed{\mathcal{Q}_{xx}(0) \le \frac{\omega_p\sqrt{\epsilon_{\infty,xx}-1}}{8\pi e^2}.} \tag{3.33}$$

The left-hand side is a fluctuation per volume. Divide by the density n_e of the same occupied electrons to obtain the directional mean-square length $\ell_x^2 = \mathcal{Q}_{xx}(0)/n_e$:

$$\boxed{\ell_x^2 \le \frac{\sqrt{\epsilon_{\infty,xx}-1}}{2m_e\omega_p}.} \tag{3.34}$$

For an isotropic three-dimensional system, the trace length is $\ell_{\mathrm{tr}}^2 = 3\ell_x^2$. Restoring units replaces $1/(m_e\omega_p)$ by $\hbar/(m_e\omega_p)$ when ω_p is an angular frequency.
Equality in this geometric-length bound requires a single active transition energy. If the measured spectrum has a frequency cutoff, or a model retains only some bands, use its actual $\mathcal{S}^1_{L,x}$ and $\mathcal{S}^{-1}_{L,x}$ in the inequality. A two-dimensional sheet response also requires its own normalization rather than a bulk dielectric constant.

3.5 Orbital interference in a triangular unit

We can play the same game on other lattices, and the triangular one shows clearly that the relative phases between orbitals do the work. Take three equivalent orbitals $|j\rangle$, $j = 0, 1, 2$, on the corners of a triangle, and form the combinations

$$|\ell\rangle = \frac{1}{\sqrt{3}}\sum_{j=0}^{2} e^{2\pi \mathrm{i}\ell j/3}|j\rangle, \qquad \ell = 0, \pm 1. \tag{3.35}$$

The combination with equal phases plays the role of the bonding orbital, and the two chiral combinations, in which the phase winds by $\pm 2\pi/3$ from one site to the next, play the role of the antibonding ones. What happens at the center of the triangle is decided by

$$1 + e^{2\pi \mathrm{i}/3} + e^{4\pi \mathrm{i}/3} = 0. \tag{3.36}$$

At a point that receives equal amplitudes from the three sites, the equal-phase combination adds constructively and the two chiral combinations cancel. If only the bonding combination is filled, the electron lives between the atoms, and poking one atom necessarily pokes its neighbors, because the filled state contains a piece of each of them. In a crystal the Bloch phases decide which combination is selected at each momentum, so a change of the charge density in real space between Γ and a valley is a direct image of this orbital interference.

In monolayer WSe_2 the valence Wannier orbital is centered at the empty hollow site between three W atoms. Three neighboring Wannier orbitals therefore overlap at each W site (Fig. 10). At Γ their amplitudes add there. At K their Bloch phases differ by $2\pi/3$ and their sum vanishes. This explains why the tunneling maps show the valence-band local density of states concentrated near W at energies around Γ and at the hollow site near the K valley edge (Holbrook et al., 2026). The node at W follows from the threefold rotation eigenvalue of the K state and persists as long as that symmetry and representation are preserved (Ingham and Queiroz, 2026).

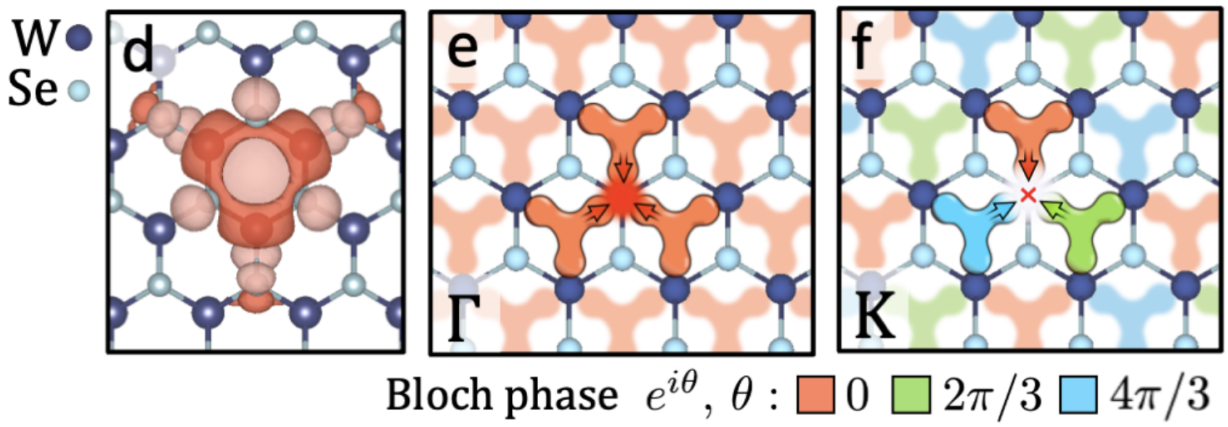


Figure 10: Orbital interference in WSe_2, adapted from Fig. 2d–f of Holbrook et al. (2026). (d) The valence Wannier orbital is centered at a hollow site. (e,f) The colors give the Bloch phases of three translated copies. At the W site where they overlap, the amplitudes add at Γ and cancel at K (cross). The tunneling map measures the resulting local spectral intensity; the phase colors belong to the schematic.

More generally, in semiconducting transition-metal dichalcogenides the metal atoms form a triangular lattice, and the bands near the gap are made of the metal orbitals d_{z^2}, $d_{x^2-y^2}$ and d_{xy}, whose hybridization is allowed by symmetry and changes with momentum; a three-orbital model captures the dispersion at the band edges and the Berry curvature near the valleys Liu et al. (2013). The metal d orbitals on neighboring sites overlap, and their relative phases determine how much valence charge builds up between the atoms. To identify an obstructed atomic limit for a chosen group of occupied bands, we must also establish that symmetry pins its Wannier centers away from the ions. The chiral combinations $d_{x^2-y^2} \pm \mathrm{i}d_{xy}$ are behind the circular optical selection rules of the valleys. The triangle isolates the interference that moves the charge in the full material.

The same delocalization gives the valleys a large Berry curvature and a large orbital magnetic moment in addition to a large metric. These quantities weigh the interband matrix elements with different powers of the transition energy, as in the moments of Lecture 2, and their magnitudes depend on the model and on the filling.

3.6 Flat bands from destructive interference

Bonding is one way to create geometry, and it requires opening a gap. Frustration is another, and it does not. Start from a square lattice with one orbital per site, which has a single band with no structure in its wave functions, so that all of its optical weight is Drude weight. In the model plotted in Fig. 11, we group four sites into a cell and reduce the hopping t_p from the plaquette site to its neighbors. At $t_p = 0$ that orbital decouples and the three connected sites form the Lieb lattice Lieb

(1989), with one hub site and two edge sites per cell. On this lattice destructive interference can stop a particle completely, even though its state extends over several atoms. With nearest-neighbor hopping and the positions of the orbitals included,

$$H(\mathbf{k}) = \begin{pmatrix} 0 & h_x & h_y \\ h_x & 0 & 0 \\ h_y & 0 & 0 \end{pmatrix}, \quad h_x = 2t_h \cos(k_x a/2), \quad h_y = 2t_h \cos(k_y a/2). \tag{3.37}$$

Away from $h_x = h_y = 0$, the vector

$$|u_0(\mathbf{k})\rangle = \frac{(0, -h_y, h_x)^T}{\sqrt{h_x^2 + h_y^2}} \tag{3.38}$$

is an exact eigenstate with zero energy for every momentum, because the two amplitudes that arrive at the hub cancel, $h_x(-h_y) + h_y h_x = 0$. This is the flat band. The other two bands have energies $\pm\sqrt{h_x^2 + h_y^2}$.

The energy of the flat band does not depend on momentum, but its wave function does, through the ratio h_x/h_y, and it changes enormously across the Brillouin zone. The projector onto the flat band therefore has a metric. In real space the state lives on the edge sites around a plaquette with alternating signs, so that the amplitudes that would leave through the hubs cancel. The electron occupies several sites and cannot move, and the reason is interference and not a lack of hopping.

At the point where the flat band touches the other two, its projector is singular. To use the metric of an isolated band we have to exclude the touching point through a controlled limit, or add a perturbation that separates the bands.

Following the square lattice as the site is disconnected shows where the optical weight goes (Fig. 11). We start with a dispersive band whose weight is all in the Drude peak. As the site is taken out, the Drude weight is progressively transferred to interband transitions, and in the Lieb limit the flat band contributes no Drude weight at all, so its response is entirely geometric. On the nearest-neighbor kagome lattice, put amplitudes of equal magnitude and alternating sign on the six sites of one hexagon. Every hop out of the hexagon has a partner of opposite sign arriving at the same site, so the electron remains on the hexagon. This is a real-space eigenstate of the flat band in Fig. 6 (Bergman et al., 2008). In Pd_5AlI_2, the orientations of the Pd and Al orbitals on a decorated checkerboard allow hopping paths to interfere, producing a nearly flat band (Devarakonda et al., 2025). The filling matters as much as the wave functions, because a large matrix element between two occupied bands contributes no absorption at zero temperature.

∴ Lieb flat band: metric, Pauli blocking and absorption

Use the hub-first basis of the Hamiltonian above. Away from the touching, write $h_x = R\cos\phi$, $h_y = R\sin\phi$, with $R = \sqrt{h_x^2 + h_y^2}$. A real orthonormal eigenbasis is

$$|u_0\rangle = (0, -\sin\phi, \cos\phi)^T, \qquad |u_\pm\rangle = \frac{1}{\sqrt{2}}(1, \pm\cos\phi, \pm\sin\phi)^T. \tag{3.39}$$

The flat-band derivative is $(0, -\cos\phi, -\sin\phi)^T \partial_\mu\phi$, orthogonal to u_0. Hence

$$g^0_{\mu\nu} = \partial_\mu\phi\, \partial_\nu\phi, \qquad \partial_x\phi = -\frac{h_y \partial_x h_x}{R^2}, \qquad \partial_y\phi = \frac{h_x \partial_y h_y}{R^2}. \tag{3.40}$$

For example,

$$g^0_{xx} = \frac{a^2 \sin^2(k_x a/2)\cos^2(k_y a/2)}{4[\cos^2(k_x a/2) + \cos^2(k_y a/2)]^2}. \tag{3.41}$$

The hopping has dropped out: the geometry depends only on the relative amplitudes, while the excitation energy R is proportional to the hopping.
Now fill the lower and flat bands completely, leaving the upper band empty (two electrons per cell for spinless fermions). Direct overlaps give

$$\langle u_\pm|\partial_\mu u_0\rangle = \mp\frac{\partial_\mu \phi}{\sqrt{2}}, \qquad \langle u_+|\partial_\mu u_-\rangle = 0. \tag{3.42}$$

Half of the flat band's metric connects it to the occupied lower band and is Pauli blocked. This is the two-electron filling of Fig. 2, with the flat band as the middle level. The factor of one half follows from the equal squared matrix elements to the two dispersive bands. The occupied-to-empty metric is therefore $g^{0+}_{\mu\nu} = g^0_{\mu\nu}/2$.
Near $\mathbf{M} = (\pi/a, \pi/a)$, set $\mathbf{q} = \mathbf{k} - \mathbf{M}$. Then $R \simeq t_h a|\mathbf{q}|$ and $g^0_{xx} \simeq q_y^2/|\mathbf{q}|^4$. The low-frequency conductivity follows by doing the radial integral:

$$\mathrm{Re}\,\sigma_{xx}(\omega) \simeq \pi e^2 \int \frac{q\,\mathrm{d}q\,\mathrm{d}\theta}{(2\pi)^2}(t_h a q)\frac{\sin^2\theta}{2q^2}\delta(\omega - t_h a q) \tag{3.43}$$

$$\longrightarrow \frac{e^2}{8} \qquad (\omega \to 0^+). \tag{3.44}$$

The four corners of a square Brillouin zone make one full neighborhood of M. This result is per spin species, for the stated filling and clean nearest-neighbor model. It implies an infrared-finite $\mathcal{S}^1_{L,x}$, a logarithmically divergent $\mathcal{S}^0_{L,x}$, and an inverse-cutoff divergence of $\mathcal{S}^{-1}_{L,x}$. Zero flat-band velocity does not eliminate absorption: the surviving transitions rotate the wave function into the empty dispersive band.

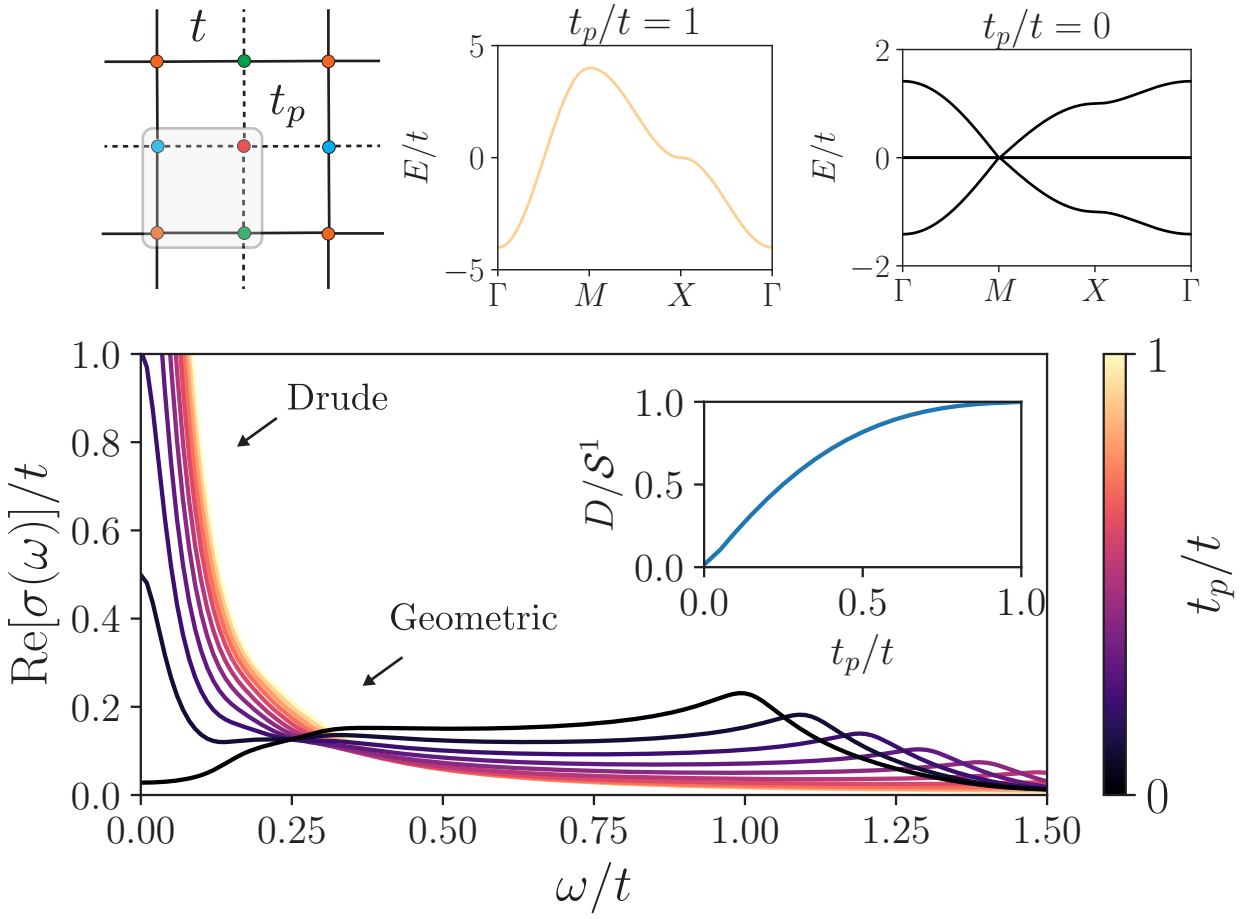


Figure 11: From Verma and Queiroz (2025a). The four-orbital model interpolates from the half-filled square lattice at $t_p = t$ to a Lieb lattice plus a decoupled plaquette orbital at $t_p = 0$. The lower panel illustrates transfer of Drude weight into interband absorption. The worked box uses the three-site Lieb Hamiltonian with the lower and flat bands completely occupied; the plotted conductivity is not a quantitative evaluation of that filling or of its $e^2/8$ limit.

3.7 Moiré length scales and what flatness leaves behind

The most effective way to create interference on a very large scale is a moiré pattern, which supplies a length L_M much larger than an atomic bond. If the texture of the wave function varies on a momentum scale $1/L_M$, then $\partial_k u$ can be of order L_M and the metric of order L_M^2: the position of an electron in a flat moiré band fluctuates over the moiré cell itself. In this sense the moiré length plays the role that the magnetic length plays in a Landau level. This is a dimensional estimate, and the actual value depends on the hybridization, on the gaps and on which bands we select.

In the square-to-Lieb interpolation the Drude peak loses weight while interband absorption survives. Even when the band is flat, an electric field can excite an electron into an empty band if the two states have a nonzero dipole matrix element. How much optical weight survives depends on those matrix elements and the excitation energies. The restricted sum can itself change as the hoppings change, and transitions to remote bands can lie outside the energy range of a flat-band model.

The spatial extent of these wave functions is also what interactions act on. Two orthogonal Wannier orbitals can have overlapping densities, so a local interaction generates matrix elements between

different configurations of pairs. One may ask how Cooper pairs made of a flat band can move at all, if the electrons do not. Think of a pair initially occupying one Wannier orbital. Where its density overlaps a neighboring orbital, an attractive interaction can give the pair an amplitude to move there even when the single-particle dispersion is flat. Such interaction-driven motion can contribute to the superfluid weight Peotta and Törmä (2015). Deriving it, or a pair mass or a spin stiffness, requires the interacting model and is beyond these lectures.

A Checks that fix the conventions

A.1 One occupied and one empty level

Let the only dipole transition have energy Δ and strength $g = |x_{01}|^2$. The formulas above reduce to

$$\mathcal{Q}_{xx}(t) = g e^{-\mathrm{i}\Delta t}, \tag{A.1}$$

$$\chi_{xx}(z) = \frac{2e^2 \Delta g}{\Delta^2 - z^2}, \tag{A.2}$$

$$\sigma_{xx}(z) = -\frac{2\mathrm{i}e^2 z \Delta g}{\Delta^2 - z^2}, \tag{A.3}$$

$$\operatorname{Re}\sigma_{xx}(\omega > 0) = \pi e^2 \Delta g \delta(\omega - \Delta). \tag{A.4}$$

The static susceptibility and positive-frequency absorption are positive, and the low-frequency longitudinal conductivity is negative imaginary with the $e^{-\mathrm{i}\omega t}$ convention. These three checks fix the relative signs.

A.2 A metal screens with a negative Drude susceptibility

From $\sigma_D(z) = \mathrm{i}D/z$ and $\sigma = -\mathrm{i}z\chi$, the Drude contribution to susceptibility is

$$\chi_D(z) = -\frac{D}{z^2}. \tag{A.5}$$

For continuum free electrons, $\epsilon(z) = 1 - \omega_p^2/z^2$, with $\omega_p^2 = 4\pi n_e e^2/m_e$. The sign is opposite to the positive static susceptibility of a bound dipole.

A.3 The diamagnetic and paramagnetic terms

In a representation where minimal coupling is $H(\mathbf{k} + e\mathbf{A})$,

$$H(\mathbf{A}) = H + eA_\mu \partial_\mu H + \frac{e^2}{2} A_\mu A_\nu \partial_\mu \partial_\nu H + \cdots . \tag{A.6}$$

The physical current is $-\partial H/\partial A_\mu$. The total paramagnetic current $j_{P,\mu}$ is the many-electron sum of $-e\,\partial_\mu H$ at zero field. Define $K_{\mu\nu} = e^2\langle \partial_\mu \partial_\nu H\rangle/V$ and the retarded paramagnetic correlator $\chi^{jj}_{\mu\nu}(t) = -\mathrm{i}\Theta(t)\langle[j_{P,\mu}(t), j_{P,\nu}(0)]\rangle/V$. Since the perturbation is $-\mathbf{j}_P \cdot \mathbf{A}$,

$$\sigma_{\mu\nu}(z) = \frac{\mathrm{i}}{z}[K_{\mu\nu} + \chi^{jj}_{\mu\nu}(z)]. \tag{A.7}$$

For an insulating longitudinal channel, $K_{xx} + \chi^{jj}_{xx}(0) = 0$. This cancellation removes a spurious Drude pole. The surviving order-z term is the bound-electron polarization derived in Lecture 2.

A.4 A single band and the occupied subspace are different choices

For an isolated band n, $Q = 1 - P_n$ includes every other band. For the optical response of a filled group, $Q = 1 - P_{\text{occ}}$ includes only empty bands. The second choice enforces Pauli blocking. At finite temperature the response uses occupation differences $f_n - f_m$; a weighted density matrix is not an idempotent projector, so identities obtained from $P^2 = P$ require modification.

B Recordings

The notes follow the three recorded lectures. Approximate time ranges:

Lecture 1, 65 minutes. Free electrons and optical weight, 02–20 min; parametric changes and projectors, 20–42 min; position fluctuations and the Bloch representation, 42–65 min.
Chalmers recording: Lecture 1.

Lecture 2, 70 minutes. Wannier spread, Landau levels and anomalous velocity, 00–19 min; velocity and the time-dependent QGT, 19–39 min; conductivity, expansions and sum rules, 39–70 min.
Chalmers recording: Lecture 2.

Lecture 3, 69 minutes. Completing the f-sum derivation, 00–13 min; material examples, bonding, orbital interference and flat bands, 13–55 min; discussion, 55–69 min.
Chalmers recording: Lecture 3.

References

Doron L. Bergman, Congjun Wu, and Leon Balents. Band touching from real-space topology in frustrated hopping models. *Physical Review B*, 78:125104, 2008.

M. V. Berry. Quantal Phase Factors Accompanying Adiabatic Changes. *Proceedings of the Royal Society of London Series A*, 392:45–57, 1984.

E. I. Blount. Formalisms of Band Theory. *Solid State Physics*, 13:305–373, 1962.

Barry Bradlyn, L. Elcoro, Jennifer Cano, M. G. Vergniory, Zhijun Wang, C. Felser, M. I. Aroyo, and B. Andrei Bernevig. Topological quantum chemistry. *Nature*, 547:298–305, 2017.

Aravind Devarakonda, Christie S. Koay, Daniel G. Chica, Morgan Thinel, Asish K. Kundu, Zhi Lin, Alexandru B. Georgescu, Sebastian Rossi, Sae Young Han, Michael E. Ziebel, Madisen A. Holbrook, Anil Rajapitamahuni, Elio Vescovo, Kenji Watanabe, Takashi Taniguchi, Milan Delor, Xiaoyang Zhu, Abhay N. Pasupathy, Raquel Queiroz, Cory R. Dean, and Xavier Roy. Frustrated electron hopping from the orbital configuration in a two-dimensional lattice. *Nature Physics*, 21:1260–1266, 2025.

Madisen Holbrook, Julian Ingham, Daniel Kaplan, Luke N. Holtzman, Brenna Bierman, Bowen Hou, Nicholas Olsen, Luca Nashabeh, Yiliu Li, Song Liu, Xiaoyang Zhu, Diana Y. Qiu, Daniel Rhodes, Katayun Barmak, James C. Hone, Raquel Queiroz, and Abhay N. Pasupathy. Real-space imaging of the band topology of transition metal dichalcogenides. *Nature Physics*, 22:680–685, 2026.

Julian Ingham and Raquel Queiroz. Real-space imaging of band topology via wavefunction zeros. arXiv:2607.21699, 2026.

Robert Karplus and J. M. Luttinger. Hall Effect in Ferromagnetics. *Physical Review*, 95:1154–1160, 1954.

Walter Kohn. Cyclotron Resonance and de Haas-van Alphen Oscillations of an Interacting Electron Gas. *Physical Review*, 123:1242–1244, 1961.

Walter Kohn. Theory of the Insulating State. *Physical Review*, 133(1A):A171–A181, 1964.

Ilia Komissarov, Tobias Holder, and Raquel Queiroz. The quantum geometric origin of capacitance in insulators. *Nature Communications*, 15:4621, 2024.

Ryogo Kubo. Statistical-Mechanical Theory of Irreversible Processes. I. *Journal of the Physical Society of Japan*, 12:570–586, 1957.

W. Kuhn. Über die Gesamtstärke der von einem Zustande ausgehenden Absorptionslinien. *Zeitschrift für Physik*, 33:408–412, 1925.

Elliott H. Lieb. Two theorems on the Hubbard model. *Physical Review Letters*, 62:1201–1204, 1989.

Gui-Bin Liu, Wen-Yu Shan, Yugui Yao, Wang Yao, and Di Xiao. Three-band tight-binding model for monolayers of group-VIB transition metal dichalcogenides. *Physical Review B*, 88:085433, 2013.

Nicola Marzari and David Vanderbilt. Maximally localized generalized Wannier functions for composite energy bands. *Physical Review B*, 56:12847–12865, 1997.

Yugo Onishi and Liang Fu. Quantum weight: A fundamental property of quantum many-body systems. *Physical Review Research*, 7:023158, 2025.

David R. Penn. Wave-Number-Dependent Dielectric Function of Semiconductors. *Physical Review*, 128:2093–2097, 1962.

Sebastiano Peotta and Päivi Törmä. Superfluidity in topologically nontrivial flat bands. *Nature Communications*, 6:8944, 2015.

J. P. Provost and G. Vallee. Riemannian structure on manifolds of quantum states. *Communications in Mathematical Physics*, 76:289–301, 1980.

F. Reiche and W. Thomas. Über die Zahl der Dispersionselektronen, die einem stationären Zustand zugeordnet sind. *Zeitschrift für Physik*, 34:510–525, 1925.

M. J. Rice and E. J. Mele. Elementary Excitations of a Linearly Conjugated Diatomic Polymer. *Physical Review Letters*, 49:1455–1459, 1982.

Rahul Roy. Band geometry of fractional topological insulators. *Physical Review B*, 90:165139, 2014.

Ivo Souza and David Vanderbilt. Dichroic f-sum rule and the orbital magnetization of crystals. *Physical Review B*, 77:054438, 2008.

Ivo Souza, Tim Wilkens, and Richard M. Martin. Polarization and localization in insulators: Generating function approach. *Physical Review B*, 62:1666–1683, 2000.

Ivo Souza, Richard M. Martin, and Massimiliano Stengel. Optical bounds on many-electron localization. *SciPost Physics*, 18:127, 2025.

D. J. Thouless, M. Kohmoto, M. P. Nightingale, and M. den Nijs. Quantized Hall Conductance in a Two-Dimensional Periodic Potential. *Physical Review Letters*, 49:405–408, 1982.

Duc Thanh Tran, Alexandre Dauphin, Adolfo G. Grushin, Peter Zoller, and Nathan Goldman. Probing topology by "heating": Quantized circular dichroism in ultracold atoms. *Science Advances*, 3:e1701207, 2017.

Nishchhal Verma and Raquel Queiroz. Instantaneous response and quantum geometry of insulators. *Proceedings of the National Academy of Sciences*, 122:e2405837122, 2025a.

Nishchhal Verma and Raquel Queiroz. Framework to Measure Quantum Metric from Step Response. *Physical Review Letters*, 134:106403, 2025b.

Nishchhal Verma and Raquel Queiroz. Long and short time linear response of metals: a geometric approach. *arXiv e-prints*, 2026.

Liang Wu, M. Salehi, N. Koirala, J. Moon, S. Oh, and N. P. Armitage. Quantized Faraday and Kerr rotation and axion electrodynamics of a 3D topological insulator. *Science*, 354:1124–1127, 2016.

Di Xiao, Ming-Che Chang, and Qian Niu. Berry phase effects on electronic properties. *Reviews of Modern Physics*, 82:1959–2007, 2010.